JMR Journal of Meteorological Research

Springer PMJ

**High-Resolution Projections of Mean and Extreme Precipitation over China by Two Regional Climate Models**

Zhiyu JIANG, Zhan TIAN, Guangtao DONG, Laixiang SUN, Peiqun ZHANG, Erasmo BUONOMO, Dongli FAN

**Citation:** Jiang, Z. Y., Z. Tian, G. T. Dong, et al., 2020: High-resolution projections of mean and extreme precipitation over China by two regional climate models. *J. Meteor. Res.*, **34**(5), 1–22, doi: 10.1007/s13351-020-9208-5

View online: http://jmr.cmsjournal.net/article/doi/10.1007/s13351-020-9208-5

# High-Resolution Projections of Mean and Extreme Precipitation over China by Two Regional Climate Models

Zhiyu JIANG[1,2,3], Zhan TIAN[3], Guangtao DONG[2,4*], Laixiang SUN[5,6], Peiqun ZHANG[7], Erasmo BUONOMO[8], and Dongli FAN[1]

1 *Shanghai Institute of Technology*, *Shanghai* 201400, *China*
2 *Shanghai Climate Center*, *Shanghai* 200030, *China*
3 *School of Environmental Science and Engineering*, *Southern University of Science and Technology*, *Shenzhen* 518055, *China*
4 *Key Laboratory of Cities' Mitigation and Adaptation to Climate Change in Shanghai*, *China Meteorological Administration*, *Shanghai* 200030, *China*
5 *Department of Geographical Sciences*, *University of Maryland*, *College Park*, *MD* 20742, *USA*
6 *School of Finance and Management*, *SOAS University of London*, *London WC1H 0XG*, *UK*
7 *Beijing Climate Center*, *Beijing* 100081, *China*
8 *Met Office Hadley Centre*, *Devon*, *EX1 3PB*, *United Kingdom*

(Received December 27, 2019; in final form June 13, 2020)

ABSTRACT

In this research, we employ two regional climate models (RCMs), which are RegCM4(无全称) and PRECIS(无全称) with a horizontal grid spacing of 25 km, to simulate the precipitation dynamics across China for the baseline climate of 1981-2010 and two future climates of 2031-2060 and 2061-2090. The global climate model (GCM) Hadley Centre Global Environment Model version 2—Earth Systems (HadGEM2-ES) is used to drive the two RCMs. The results of baseline simulations show that the two RCMs can correct the obvious underestimation of light rain below 5 mm day-1 and the overestimation of precipitation above 5mm day-1 in Northwest China and the Qinghai-Tibet Plateau, as being produced by the driving GCM. While PRECIS outperforms RegCM4 in simulating annual precipitation and wet days in several sub-regions of Northwest China, its underperformance shows up in Eastern China. For extreme precipitation, the two RCMs provide a more accurate simulation of continuous wet days (CWD) with reduced biases and more realistic spatial patterns compared to their driving GCM. For other extreme precipitation indices, the RCM simulations show limited benefit except for an improved performance in some localized regions. The future projections of the two RCMs show an increase in the annual precipitation amount and the intensity of extreme precipitation events in most regions. Most areas of Southeast China will experience fewer number of wet days, especially in summer, but more precipitation per wet day (≥ 30 mm day-1). By contrast, number of wet-days will increase in Qinghai-Tibet Plateau and some areas of Northern China. The increase in both the maximum precipitation for 5 consecutive days and the regional extreme precipitation will lead to a higher risk of flooding events. The findings of this study can facilitate the efforts of climate service institutions and government agencies to improve climate services and to make climate-smart decisions.

**Key words:** Climate change, extreme precipitation, dynamical downscaling, different RCMs, Coordinated Regional Downscaling Experiment (CORDEX)

**Citation:** Jiang, Z. Y., Z. Tian, G. T. Dong, et al., 2020: High-resolution projections of mean and extreme precipitation over China by two regional climate models. *J. Meteor. Res.*, **34**(5), 1–22, doi: 10.1007/s13351-020-9208-5.

## 1. Introduction

China has been vulnerable to various hazards caused by extreme weather/climate events. The observed cli-

Supported by the National Key Research and Development Program of China (2018YFA0606204), National Natural Science Foundation of China (51761135024 and 41671113), UK–China Research & Innovation Partnership Fund through the Met Office Climate Science for Service Partnership (CSSP) China as part of the Newton Fund (P106409), and Social Development Project of STCSM(全拼）(19DZ1201500).

*Corresponding author: gtdong@163.com.

mate change in past few decades has exacerbated the severity of extreme events such as floods and droughts and this exacerbation may continue into the next decades owing to future climate change (Zhou et al., 2018; Liang et al., 2019). As the monsoon region accounts for about 60% of the Asian continent, the East Asian summer monsoon is the most distinctive climate feature in China (Ding and Chan, 2005本条文献在文后文献中未体现). East Asian summer monsoon anomalies can lead to floods and droughts, which greatly affect the livelihoods of more than 1 billion people in the region (Webster et al., 1998; Gu et al., 2015; Yu et al., 2018). Using the Coupled Model Intercomparison Project 5 (CMIP5) monthly surface precipitation data at the 0.5° × 0.5° grid degree from 2011 to 2099 and the corresponding reanalysis data for 1981-2010, Liang et al. (2019) showed that flood hazards as measured by the changes in flood accumulation (ΔFA) will increase by a large margin in Guangdong, Hainan, Guangxi, and Fujian provinces in South China, and floods in Southeast China and the northern Yunnan Province may become more severe. Floods and droughts may occur in the same year, and may also occur alternately in consecutive years, meaning that an area may be at risk for both drought and flood in one year or in consecutive years. Therefore, there is an urgent demand for more accurate assessments of flood and drought risks brought about by future climate change, beyond the coarse assessment based on the global climate models (GCMs) of CMIP5.

This urgent demand has stimulated a growing number of publications on simulating and predicting extreme precipitation in China (see, e.g., Chen, 2013; Wang and Chen, 2014; Li et al., 2016; Sun et al., 2016; Gu et al., 2018). It has been acknowledged that the main solution is to either develop high-resolution GCMs or nest high-resolution regional climate models (RCMs) into low-resolution GCMs. Compared with low-resolution GCMs, high-resolution GCMs are more skillful at simulating extreme precipitation (Zhang et al., 2016; Duan et al., 2019), and capable of providing more realistic treatment of associated physical mechanisms (Chen et al., 2018). However, even relatively high resolution GCMs at present are still not ideal in studying the changes of temperature and precipitation extremes, because the resolution is not high enough to fully represent many important local features, such as the mesoscale terrain and heterogenous land covers and land uses. The alternative way of nesting high-resolution RCMs into low-resolution GCMs is to run a limited area RCM over a selected domain of interest for long continuous simulation times driven by initial and time‐dependent meteorological lateral boundary conditions (LBC) obtained either from global reanalyses of observations or by GCM simulations (Giorgi, 2019). This approach is commonly referred to as dynamical downscaling. RCMs can account for the effects of sub‐GCM grid scale forcings and processes associated with complex topography, coastlines, inland bodies of water and land cover distribution, or dynamical processes occurring at the mesoscale. These advantages enable RCMs to produce better results than GCMs (Feser et al., 2011), and also to directly improve the resolution of GCMs with less demand for computing resources. As a consequence, this approach has been increasingly used in predicting extreme events at a regional scale.

Though RCMs have been widely used for more refined historical simulations and future projections, their applications in East Asia and China have still exhibited the following shortcomings: (1) Most of publications only used one GCM to drive a single RCM, making it difficult to characterize the modeling uncertainties (Niu et al., 2017; Zhang et al., 2017; Gu et al., 2018; Li et al., 2018本条文献指代信息不明确; Chen and Gao, 2019). (2) Some studies used multiple GCMs to drive a single RCM, and some used a single GCM to drive multiple RCMs. Hui et al. (2018a, b) were among the first who employed two GCMs to drive two RCMs. However, only a short time slice was simulated in these studies, which fail to cover the whole 21st century. Besides, the resolution of RCMs in these studies were 50 km or above (Yang et al., 2016; Hui et al., 2018a, b; Wei et al., 2019).

Recent works on 25 km-resolution RCMs showed their improved ability in reproducing the regional annual cycle and the frequencies and intensities of daily precipitation than RCMs with 50-km resolution (Zhu et al., 2017; Zhang et al., 2017; Guo et al., 2018; Lu et al., 2019). At present, however, there is a lack of RCM simulations over China that are able to meet all of the following three requirements: (1) Using a GCM to drive two different RCMs; (2) working with two or more scenarios of climate warming and producing simulations for the whole 21st century; (3) having a resolution of 25 km or finer. Our study intends to fill this important niche. In more detail, our study evaluates the ability of two RCMs, RegCM4, and PRECIS, being driven by Hadley Centre Global Environment Model version 2—Earth Systems (HadGEM2-ES) under two scenarios of global warming, in simulating the mean and extreme climate by comparing with the observation, and then examine their projections of future precipitation. With an emphasis on extreme precipitation, the finding in the study will bridge the gap between the climate information developed by scientists and service providers and the practical needs of

end-users, such as national and regional climate institutions (decision makers), water conservancy department and farmers.

The rest of the paper is organized as follows. Section 2 provides details of the experiment design, reference datasets and evaluation methods. Section 3 presents the evaluation of RCMs in simulating the regional climate, and Projections of future climate. Finally, Section 4 summarizes.

## 2. Data and methods

### 2.1 *Observed data*

The observation data used for validation is the CN05.1 gridded dataset (Wu and Gao, 2013). The dataset is based on observational data from 2416 meteorological stations in China with a horizontal resolution of 0.25° × 0.25° (longitude × latitude). The dataset includes daily precipitation, daily average surface temperature, maximum temperature, minimum temperature, evaporation, average wind speed, relative humidity and other meteorological variables from 1961 to 2012. It was constructed using the 'anomaly approach' during the interpolation, as performed by Xu et al. (2009). Anomaly approach calculates a gridded climatology first, then adds a gridded daily anomaly to the climatology to obtain the final data set. This dataset has been widely used in model verifications (e.g. Gao et al., 2013; Zhou et al., 2014, Yun et al., 2020).

### 2.2 *Models*

The GCM used here is the HadGEM2-ES, which is used for the core climate simulations for CMIP5 (Shi et al., 2018). HadGEM2-ES is a coupled AOGCM with the atmospheric resolution of N96 (1.875° × 1.25°) and 38 vertical levels, and an ocean resolution of 1° (increasing to 1/3° at the equator) and 40 vertical levels (Jones et al., 2011). HadGEM2-ES has added terrestrial and ocean ecosystems and gas-phase tropospheric chemistry to the latest version, and is considered as the best model in simulating most variables especially surface conditions and atmospheric circulation (Zhu et al., 2017).

There are two RCMs used in this study. PRECIS is a regional climate simulation system developed by the Hadley Climate Prediction and Research Center of the UK Meteorological Administration based on GCM-HadCM3 with a horizontal grid spacing of 50 or 25 km, corresponding to a time-integration step of 5 and 2.5 minutes, respectively. This study uses the latest version of PRECIS 2.0.0 (Wilson et al., 2015).

Based on the comparative analysis of a large number of experiments under RegCM4.4 driven by reanalysis data (Gao et al., 2016), this study selected a combined parameterization with better simulation effect for China: the atmospheric radiative transfer is computed using the radiation package from the NCAR Community Climate Model CCM3 (Kiehl et al., 1998), the planetary boundary layer is described by Holtslag et al. (1990), resolvable scale precipitation is represented by the SUBEX(无全称) parameterization of Pal et al. (2007), convection is represented by the Emanuel scheme and the version of the CLM(无全称) land surface scheme used here is CLM3.5. The land cover data used in the experiment are based on 1:1 million vegetation map of China (Han et al., 2015). This version of RegCM4 has been applied in the second phase of the Coordinated Regional Climate Downscaling Experiment - East Asia (CORDEX-EA-II), including historical simulation assessment (Han et al., 2016; Gao et al., 2017) and future climate change Projection (Han et al., 2017; Zhang et al., 2017; Gao et al., 2018; Shi et al., 2018; Zhou et al., 2018). RegCM4 data is provided by the National Climate Center (NCC). Before the long-term numerical simulation, NCC and Gao et al. (2017, 2018) combined and optimized different parameterization schemes, and finally determined a set of suitable parameterization schemes for the simulations in East Asia. Table 1 presents a summary of the experimental design for both RCMs.

Like CORDEX-EA-II framework (CORDEX; Giorgi et al., 2009), the simulation domain (Fig. 1) covers most of Asia, the western Pacific, the Bay of Bengal and the South China Sea with a horizontal grid spacing of 25 km (RegCM4) or 0.22° (PRECIS).

HadGEM2-ES provides the LBC for the two RCMs to produce the high-resolution historical simulation and future projections. The historical simulations are conducted from 1979-12-01 to 2005-12-30, with the first month as the model spin-up time. For the projection of the future climate, RCP4.5 and RCP8.5(RCP无全称) are selected to drive the model. The simulations of the future climate are conducted from 2005-12-01 to 2098-12-30, again with the first month used as the model spin-up time

**Table 1.** Experiment design for the downscaling simulations表格中很多缩写无全称, 需要在表下备注

| 排版请录入: 缺? | PRECIS | RegCM4 |
|---|---|---|
| Governing equations | Hydrostatic | Hydrostatic |
| Initial and boundary conditions | HadGEM2-ES | HadGEM2-ES |
| Cumulus convection | Tiedtke | MIT-Emanuel |
| Microphysics | Seifert and Beheng | SUBEX |
| Radiation | Ritter and Geleyn | Modified CCM3 |
| Land surface | TERRA_ML | CLM |
| Planet boundary layer | TKE level 2.5 | Modified Holtslag |
| Horizontal resolution | 0.22° (~25km) | 25 km |

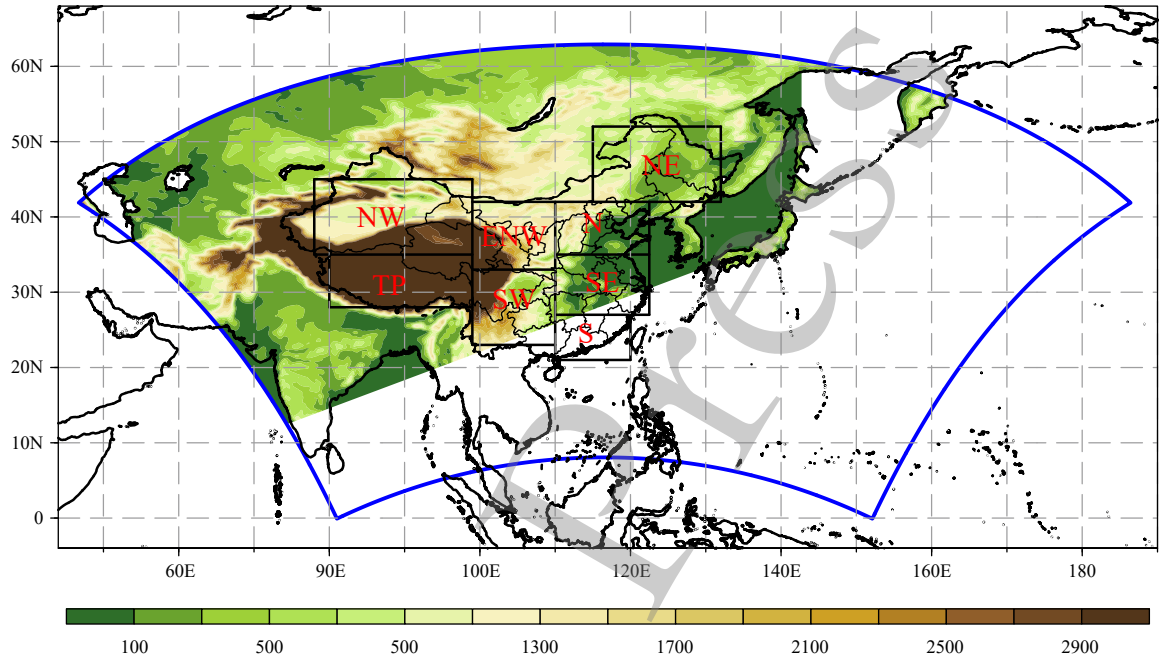


**Fig. 1.** The simulation domain and the 8 sub-regions in RCMs: Northwest (NW), 78E~99E, 35N~45N; Qinghai-Tibet Platea (TP), 80°~99°E, 28°~45°N; Eastern Northwest (ENW), 99°~110°E, 34°~42°N; Southwest (SW), 99°~100°E, 24°~34°N; Northeast (NE) 115°~132°E, 42°~52°N; North China (N) 110°~122.5°E, 35°~42°N; Southeast (SE) 110°~122.5°E, 27°~35°N; South China (S) 110°~120°E, 21°~27°N.编稿时图题中的缩写需要注意.

that are not include in the analysis. In order to fully cover decadal variability, an average of 30 years usually represents a time frame in climate model assessments. The period from 1981 to 2010, in which 2006-2010 is under the RCP4.5 scenario, is used as the historical reference period to make up the 30 years (the carbon dioxide content in this period is still almost the As in the historical period from 1980 to 2005). Therefore, in the comparison analysis of this research, the baseline is 1981-2010, the future periods include mid-twenty-first century (2031–2060, i.e., the 2050s), and late-twenty-first century (2061–2090, i.e., the 2080s).

### 2.3 *Key indicators for performance assessment*

We adopt key precipitation indicators recommended by the Expert Team on Climate Change Detection and Indexes to assess the performance of the two RCM models in terms of mean and extreme precipitation, as shown in Table 2.

The added value (AV) is used to evaluate the improvement with downscaling (Hui et al., 2018a). The formula proposed by Di Luca et al. (2013) and adapted by Dosio et al. (2015) is used here:

$$\mathrm{AV} = \frac{(X_{\mathrm{GCM}} - X_{\mathrm{OBS}})^2 - (X_{\mathrm{RCM}} - X_{\mathrm{OBS}})^2}{\mathrm{Max}\left[(X_{\mathrm{GCM}} - X_{\mathrm{OBS}})^2, (X_{\mathrm{RCM}} - X_{\mathrm{OBS}})^2\right]}, \quad (1)$$

where $X$ represents the spatial fields in different datasets. AV is positive when the RCM's squared error is smaller than its forcing GCM, which means that the RCM improves the GCM's results. The normalization is introduced here, thus, $-1 \leqslant \mathrm{AV} \leqslant 1$.

To quantify the performance of RCMs, the common statistical measures—the root mean square error (RMSE) and the spatial correlation coefficient (CORR) between observations and simulations —are calculated. The equations are as follows.

**Table 2.** Definitions of precipitation indexes

| Index | Indicator name | Definition | Unit |
|---|---|---|---|
| PRCPTOT | Total wet-day precipitation | Total precipitation with daily rainfall ($R$) >1 mm in a year | mm |
| R1mm | Number of wet days | Number of days with daily $R$ > 1 mm in a year | day |
| SDII | Simple daily intensity index | Total rainfall divided by total wet days in a year | mm day$^{-1}$ |
| R95p | Extreme precipitation amount | Annual total precipitation when $R$ > 95th percentile | mm |
| R95t (R95pTOT) | Extreme precipitation proportion | Proportion of $R$ >95th percentile in all rainfall events | % |
| Rx5day | Maximum precipitation for 5 consecutive days | Maximum amount of precipitation for 5 consecutive days in a year | mm |
| CWD | Consecutive wet days | Maximum number of consecutive days with daily $R$ > 1 mm in a year | day |
| CDD | Consecutive dry days | Maximum number of consecutive days without precipitation in a year | day |

$$\mathrm{RMSE} = \sqrt{\frac{\sum (m_i - o_i)^2}{N_i}}, \tag{2}$$

$$\mathrm{CORR} = \frac{\sum (m_i - \bar{m}) \bullet \sum (o_i - \bar{o})}{\sqrt{\sum (m_i - \bar{m})^2 \bullet \sum (o_i - \bar{o})^2}}, \tag{3}$$

where $\bar{m}$ stands for the spatially averaged value from model outputs, $\bar{o}$ for the spatially averaged value from reanalysis/observations and $N_i$ for the number of grid points.

## 3. Results

### 3.1 *Evaluation of historical simulation*

#### 3.1.1 *Climatology*

The observed and simulated 30-year average total wet-day precipitation (PRCPTOT) and number of wet days (R1mm) over 1981-2010 are displayed in Figs. 2, 3.

In terms of 30-average total wet-day precipitation over 1981-2010, the simulations are consistent with the observations in terms of spatial patterns in which the precipitation decreases from the southeast coast to the northwest inland. All models perform better in the eastern China than in the western part of the country in terms of percentage bias. HadGEM2-ES has wet biases within 40% of the observation in NE and N, a small negative bias within 20% in SE, and a large wet bias in NW, ENW, and TP. The comparison across maps e-g in Fig. 2 shows that GCM overestimates the precipitation in the middle and lower reaches of the Yangtze River and its south areas, such biases are significantly reduced in RCM simulations, especially in PRECIS simulations. It may be attributed to a better representation of low-level water vapor flux and vorticity in RCMs. In the NE, GCM, and RCMs all overestimate the precipitation because of the positive bias of low-level potential vorticity in RCMs and their forcing GCM, and the bias in RCMs is larger, especially in RegCM4. By calculating AV for the wet-day precipitation, it is revealed that RCMs improve GCM mainly in SE, TP, and parts of NW.

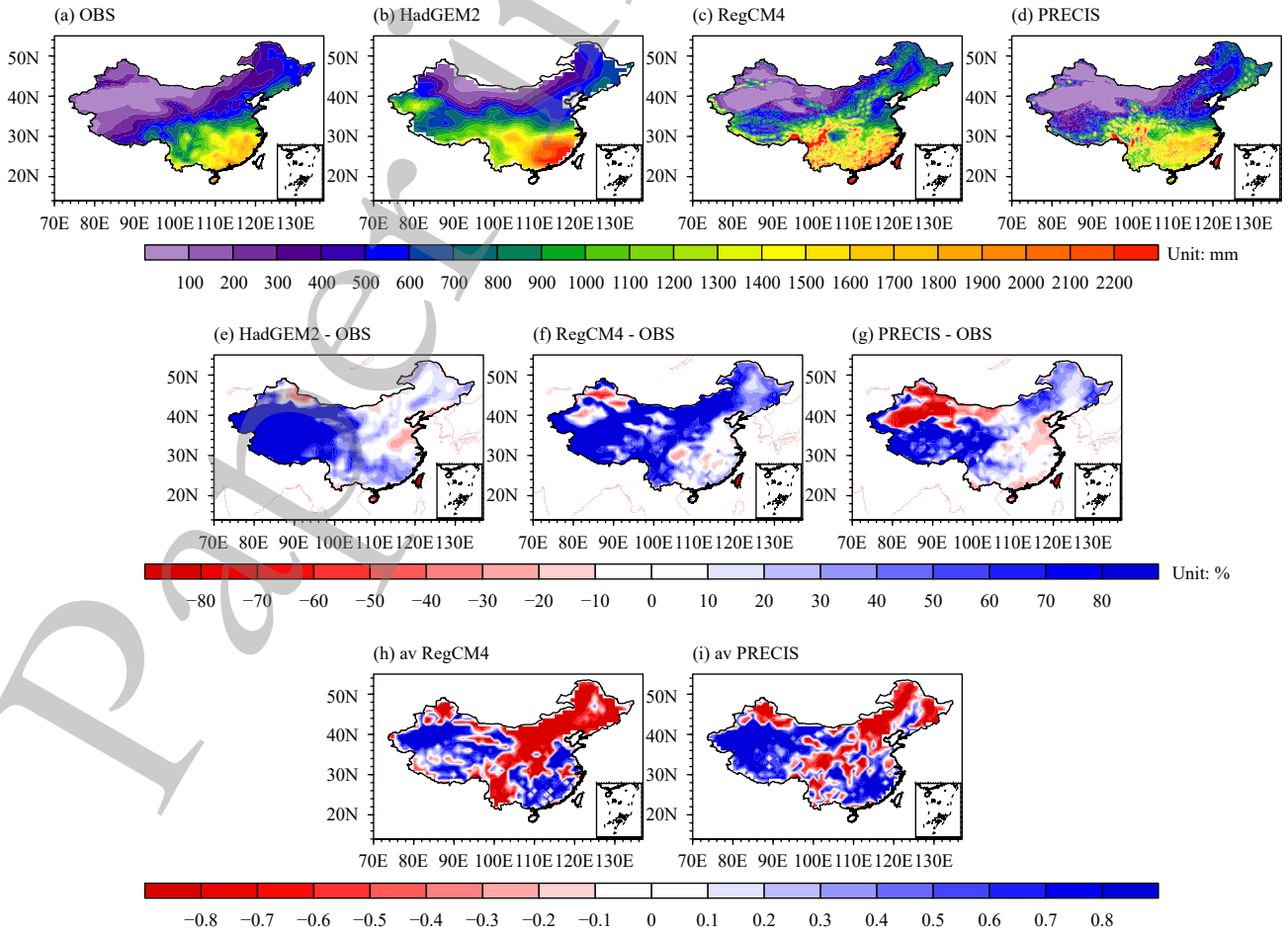


**Fig. 2.** (a–d) Observed and simulated 30-average total wet-day precipitation over 1981-2010 by each model (mm); (e–g) differences between the simulation and the observation (%); and (h–i) AVs of RCMs versus AV of GCM.

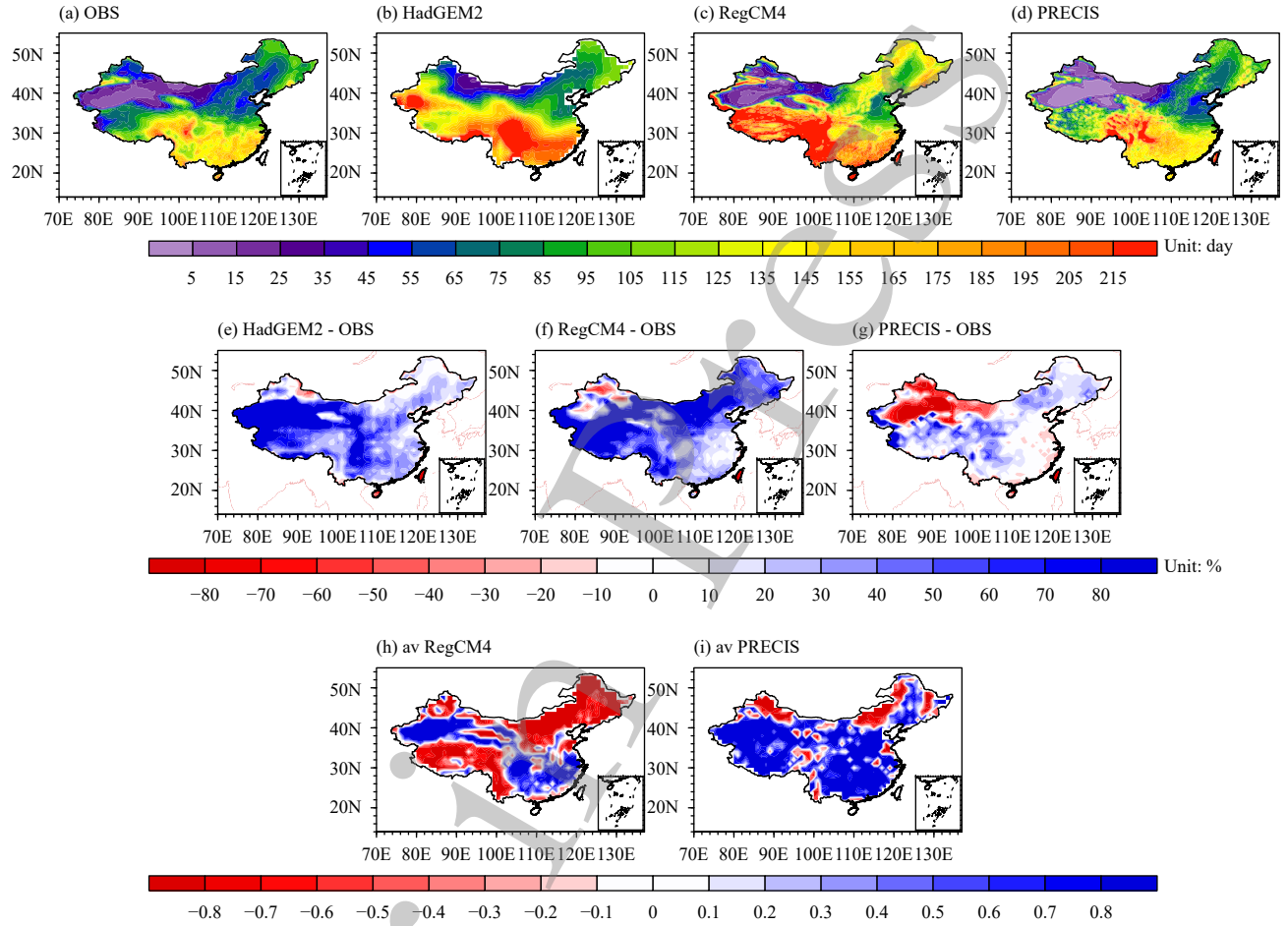


**Fig. 3.** As in Fig. 2, but for number of wet-days (R1mm).

In terms of the number of wet-days, HadGEM2-ES and RegCM4 overestimate it across the whole country, especially in TP and SW, and the smallest biases (less than 20%) appear in SE and S. At the same time, both the models underestimate the number of wet days in some parts of NW. In contrast, the PRECIS simulation is better. The biases in most of SE and S are below10%, and the biases in NE, SW and TP are also significantly smaller than the other two models. It is worth noting that PRECIS underestimates the number of wet days in large areas of NW, which coincides with its underestimation of the wet-day precipitation. It can be seen from Fig. 3 that for number of wet days, PRECIS has a positive AV in most parts of China, clearly indicating its better performance than the GCM. However, it is worth noting that RegCM4 degrades the GCM's performance in TP and SW.

3.1.2 *Annual cycle*

The latitude-month distributions of precipitation and R1mmin the eastern China (100°–130°E) are shown in Fig. 4. The RMSE and CORR between the observed and simulated precipitation seasonal cycles are given in Tables 3 and 4. The observation indicates that the precipitation is concentrated in May–August between 22–32°N. The annual precipitation north of 37°N is relatively weak, concentrating in June–August. These spatiotemporal characteristics are captured in all simulations. However, the simulated precipitation in the vicinity of 27°N comes too early. In both HadGEM2-ES and PRECIS, the earlier occurrence of the rain belt can be seen, but it is not apparent in RegCM4. In addition, HadGEM2-ES and RegCM4 produce excessive precipitation throughout the year. As shown in Tables 3 and 4, PRECIS has successfully improved the GCM simulation in NW, TP, ENW and SW (Figs. 5a-d) by significantly increasing correlation coefficients and reducing RMSEs. Compared with HadGEM2-ES, the most significant enhancement of PRECIS occurs in the western China. Overall RegCM4 does not perform as wet as PRECIS, but it also improves HadGEM2 in NW and S (Figs. 5a, h). The observed R1mm are no more than 21 days from June to August in the vicinity of 22°N, but the models

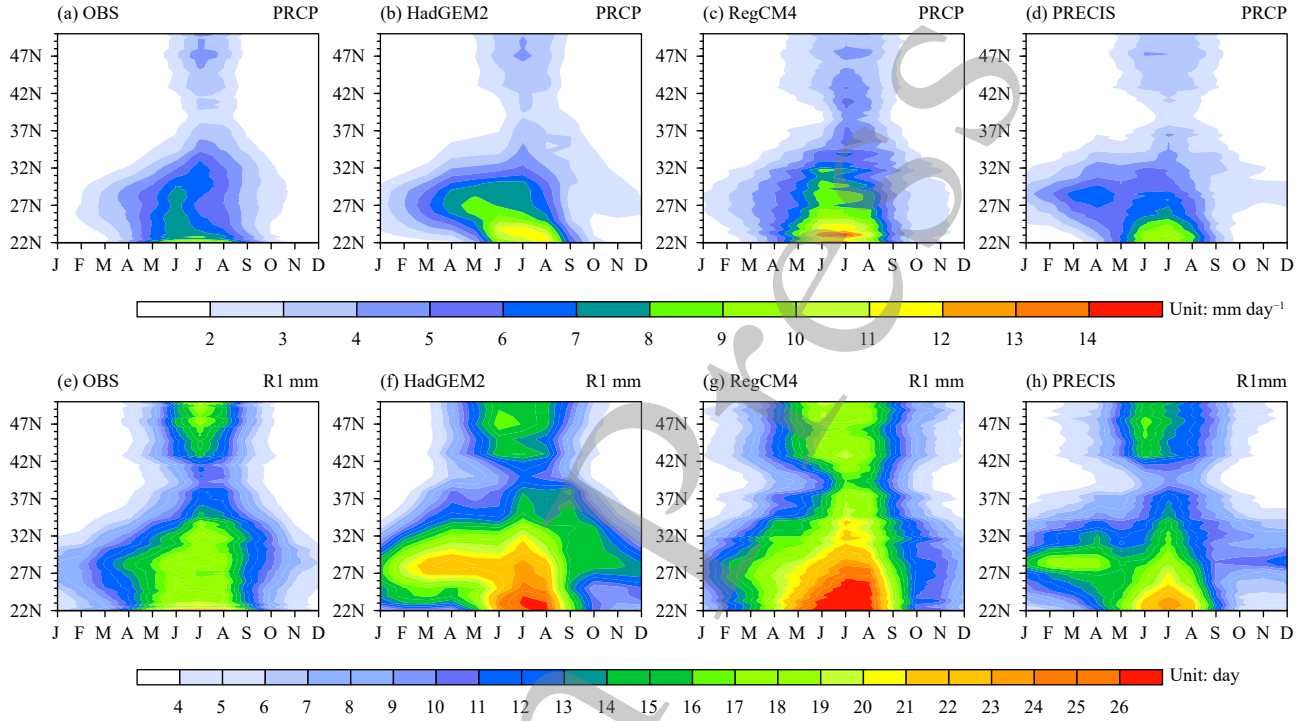


**Fig. 4.** Latitude-month cross-sections of the (a–d) observed and simulated precipitation, as well as (e–h) number of wet days (22°N–50°N,100°E–130°E).

**Table 3.** RMSE between simulations and observations for the seasonal cycle of precipitation. The statistics of the RCMs are printed in bold when they improve the driving GCMs

| Index | Model | NW | TP | ENW | SW | NE | N | SE | S |
|---|---|---|---|---|---|---|---|---|---|
| PRCPTOT (mm day$^{-1}$) | HadGEM2 | 1.347 | 1.992 | 0.601 | 1.067 | 0.362 | 0.248 | 1.073 | 1.727 |
| | PRECIS | **0.194** | **1.666** | **0.596** | **1.004** | 0.631 | 0.457 | 1.502 | **1.252** |
| | RegCM4 | **0.485** | **1.979** | 0.864 | 1.666 | 0.798 | 0.893 | **0.574** | **1.403** |
| R1mm (Day) | HadGEM2 | 6.674 | 6.534 | 3.990 | 6.627 | 2.032 | 2.118 | 3.440 | 4.967 |
| | PRECIS | **2.341** | **3.758** | **2.347** | **3.479** | 2.335 | **1.545** | **2.979** | **2.626** |
| | RegCM4 | **4.075** | 10.657 | 4.196 | **6.099** | 4.701 | 4.388 | **2.647** | 4.749 |
| SDII (mm day$^{-1}$) | HadGEM2 | 1.622 | 1.967 | 0.258 | 0.941 | 0.230 | 1.353 | 2.012 | 1.184 |
| | PRECIS | **1.417** | 2.953 | 1.779 | 1.267 | 1.302 | **0.839** | **1.914** | **0.940** |
| | RegCM4 | **0.717** | **1.671** | 0.542 | **0.929** | 0.748 | **0.806** | **1.566** | 1.580 |

**Table 4.** CORR between simulations and observations for the seasonal cycle of precipitation. The statistics of the RCMs are printed in bold when they improve the driving GCMs

| Index | Model | NW | TP | ENW | SW | NE | N | SE | S |
|---|---|---|---|---|---|---|---|---|---|
| PRCPTOT | HadGEM2 | 0.895 | 0.952 | 0.902 | 0.977 | 0.976 | 0.985 | 0.832 | 0.963 |
| | PRECIS | **0.899** | **0.992** | **0.935** | **0.982** | 0.945 | 0.951 | 0.571 | 0.876 |
| | RegCM4 | 0.864 | **0.964** | **0.989** | **0.989** | 0.967 | **0.992** | **0.966** | 0.957 |
| R1mm | HadGEM2 | 0.834 | 0.919 | 0.855 | 0.952 | 0.955 | 0.968 | 0.864 | 0.897 |
| | PRECIS | 0.788 | **0.980** | **0.955** | **0.972** | 0.938 | 0.940 | 0.549 | 0.874 |
| | RegCM4 | 0.754 | 0.864 | **0.981** | **0.980** | 0.948 | **0.984** | **0.984** | **0.952** |
| SDII | HadGEM2 | 0.789 | 0.899 | 0.984 | 0.958 | 0.993 | 0.980 | 0.815 | 0.954 |
| | PRECIS | 0.653 | **0.918** | 0.921 | **0.962** | 0.957 | 0.954 | 0.694 | 0.915 |
| | RegCM4 | 0.718 | **0.907** | 0.977 | **0.955** | **0.993** | 0.965 | **0.819** | 0.938 |

show an occurrence higher than 21 days, with the largest number (above 26 days) in RegCM4. PRECIS improves CORR and reduces RMSEs in TP, ENW, SW and other sub-regions, while RegCM4 significantly improves the GCM in the eastern China.

3.1.3 *Frequency of precipitation intensity*

The frequency of precipitation intensity is established for different regions. Only the days whose corresponding daily precipitation ≥ 1 mm are considered. It can be seen from Fig. 6 that the frequency in each region decreases with the increase of intensity. In NW, ENW, NE and TP, the observed light-rain (1–5 mm day$^{-1}$) fre-

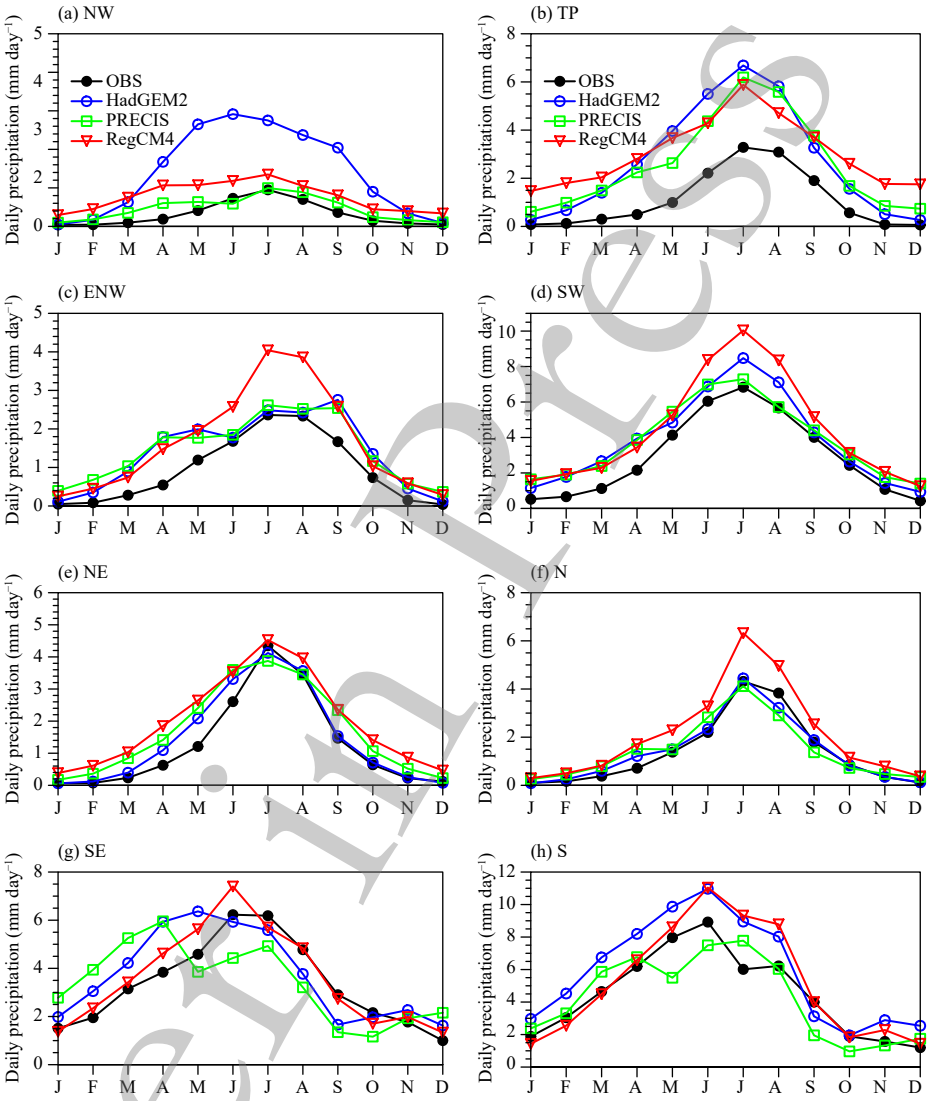


**Fig. 5.** Annual cycle of precipitation (mm day$^{-1}$) over China and the eight sub-regions during 1981–2010.

quency, usually more than 60%, is much higher than that in other regions. But there is rare heavy rain with intensity over 20 mm day$^{-1}$ in NW, ENW and TP. In SE and S, the light rain frequency is less than 50%, while the heavy rain frequency is higher. In general, GCMs and RCMs can reasonably capture the frequency distribution of precipitation in each sub-region, but there are some defects. HadGEM2-ES underestimates the light rain frequency in NW and TP, while overestimates the frequency of moderate rain (5–10 mm day$^{-1}$) in these two areas, which are greatly corrected by the two RCMs. For other sub-regions, except for the significant bias in light rain, the simulation is in good agreement with the observation.

3.1.4 *Extreme indexes*

To evaluate the models' ability in representing the spatial pattern of extreme precipitation indexes, a Taylor diagram (Taylor, 2001) is utilized to illustrate the spatial correlation, normalized standard deviation and normalized centered RMSE between the simulation and observation in Fig. 7. The models show large inconsistencies in simulating the spatial patterns of the extreme precipitation indexes in different sub-regions. The models show good correlation coefficients in most regions, as the threshold value of the correlation coefficient being at the 0.95 significance level is 0.349. With normalized standard deviations close to 1 and the normalized centered RMSEs ranging from 1 to 2, the GCM produces the batter spatial patterns in many sub-regions like TP and ENW than the RCMs in simulating extreme precipitation (Figs. 7d, e). However, RegCM4 and PRECIS improve the R95p in SE. There are large regional differences in simulation capability. The three models all overestimate Rx5day in all regions except for SE and S (figures omitted), so lower normalized centered RMSEs and

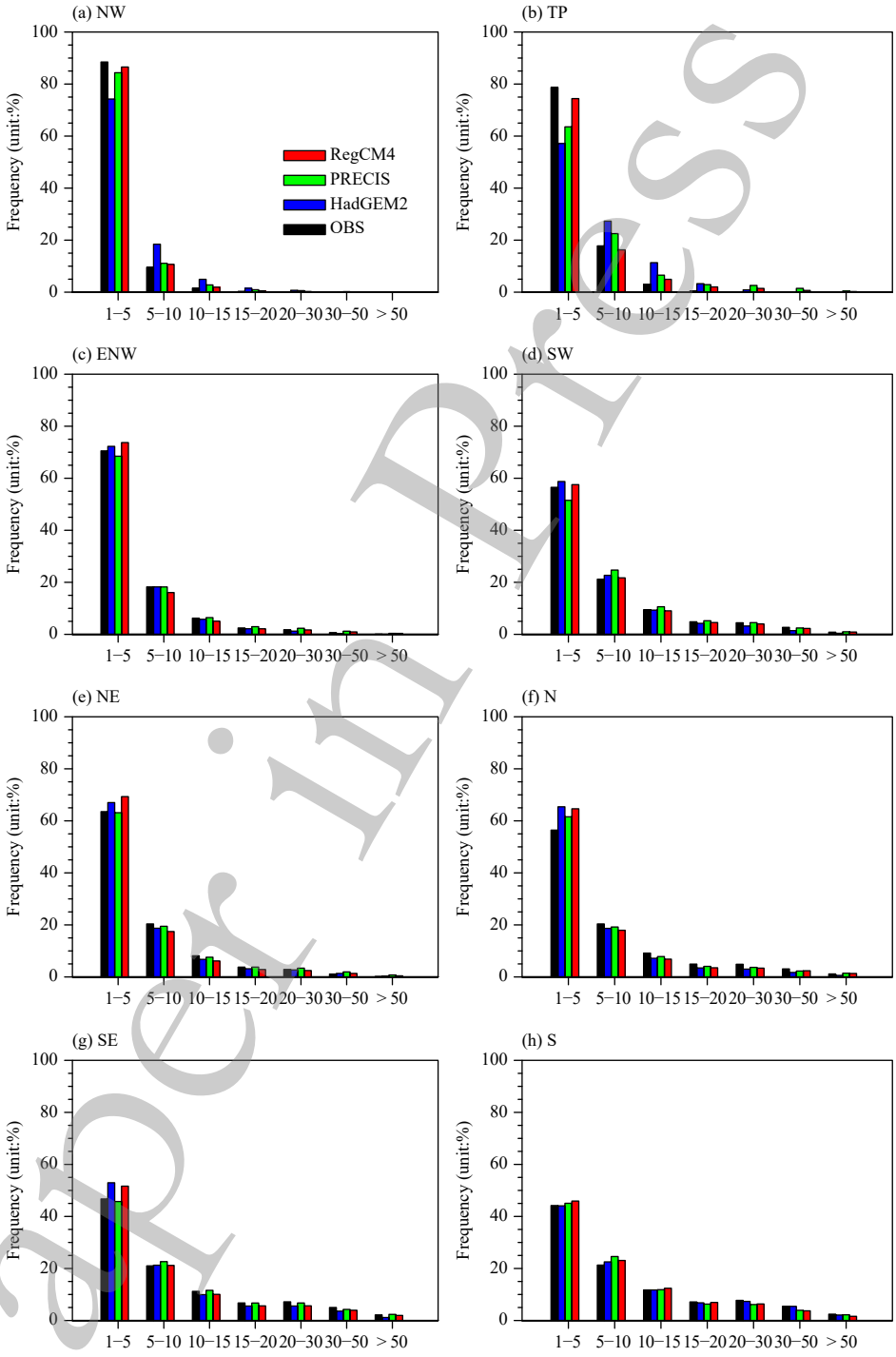


**Fig. 6.** Observed and simulated frequency of daily precipitation calculated for different sub-regions of China.

normalized standard deviations are shown in SE and S (Fig. 7f). It is worth noting that there is relatively less observed precipitation in the areas with overestimated Rx5day, thus a small absolute bias can lead to a large percent bias. PRECIS has the best performance in CWD (the longest Consecutive wet days) in almost all regions except NW, with the normalized centered RMSEs ranging from 1 to 2 and the normalized standard deviations closer to 1.

In terms of extreme indexes, RCMs have obvious better performance than GCM on CWD in most areas and in annual number of wet days (R1mm) in some regions. PRECIS improves the GCM's representation of CWD in all sub-regions, especially in Eastern China (including NE, N, SE and S). The main reason is that the number of wet days in Eastern China are larger than those observed

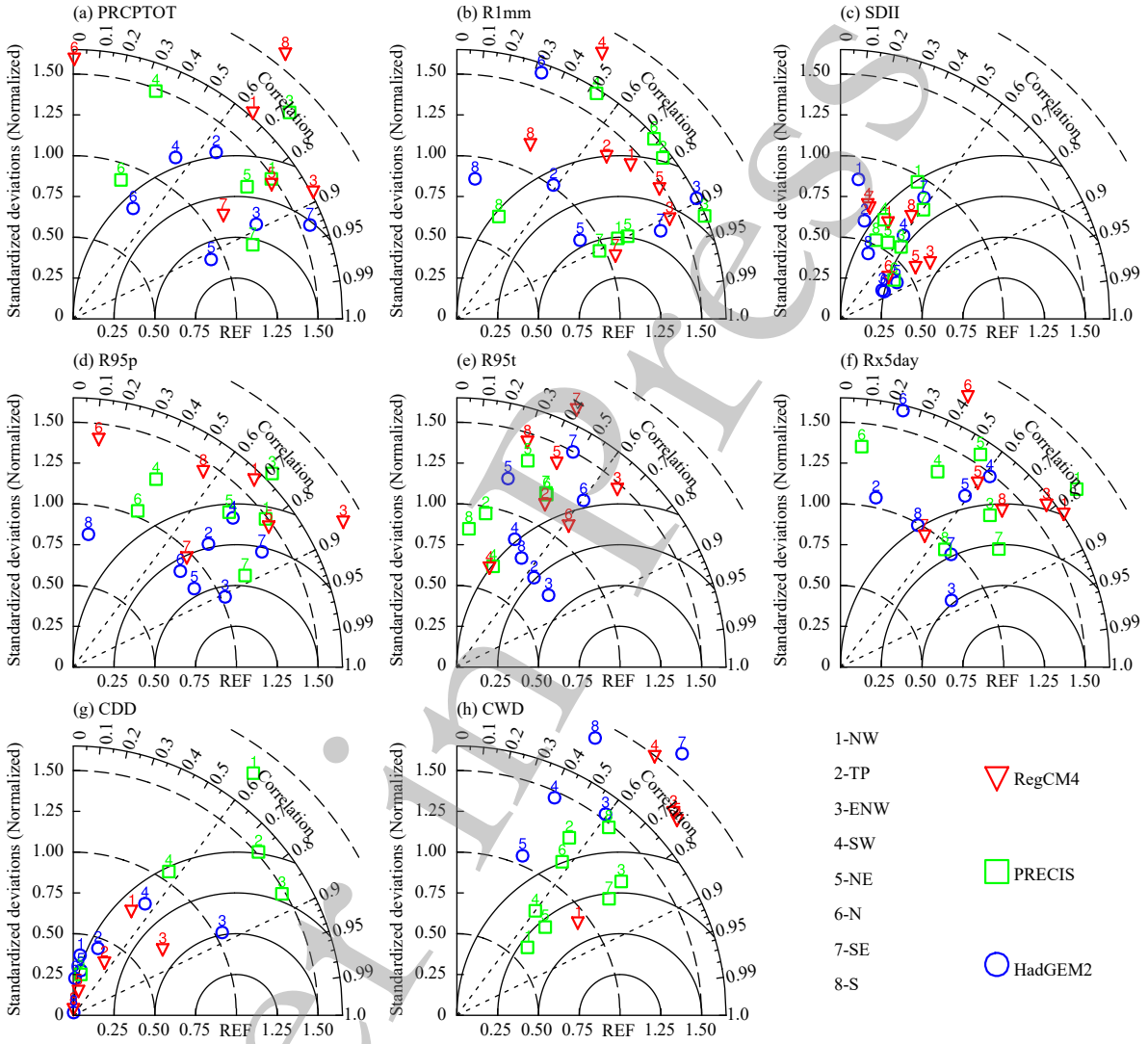


**Fig. 7.** Taylor diagram of the statistical analysis of different models in simulating the spatial pattern of different indexes in the different sub-regions of China.

(Fig. 3), which is a common problem in many other GCMs (Jiang et al., 2012本条文献在文后文献中未体现). RCM simulations of the number of wet days significantly reduced the bias of the GCM, with the reduction in PRECIS being more noticeable.

Some extreme indexes simulated by RCMs are inferior to that by GCM, such as extreme precipitation amount (R95p) in some regions. Both RCMs do not perform as well as GCM on the index R95p in SW, the main reason may rest with the topographical fluctuations in the area, and that daily extreme precipitation in steep terrain is usually larger in RCM than observation (Hui et al., 2018a). When taking probability density function (PDF) into consideration (figures omitted), RCMs simulate more realistic extreme precipitation in SW, while GCM could not simulate the strongest precipitation in this area. The two observation datasets with resolution of 0.25 degrees (CN05.1 and TRMM) have the strongest precipitation in this region up to 220 and 260mm, respectively. The tail of the PDF curve simulated by the GCM is significantly shorter, and the strongest precipitation is only 140 mm. The RCMs can simulate extreme heavy precipitation in the region, although the PDF curve tail is longer than the observation.

### 3.2 *Projection of future climate*

#### 3.2.1 *Climatology*

Figure 8 shows the annual precipitation change under the two RCP scenarios between the baseline of 1981-2010 and the 2050s and 2080s respectively. By the 2050s, the extent of annual precipitation change in most parts of the country will be within 10%, with the largest

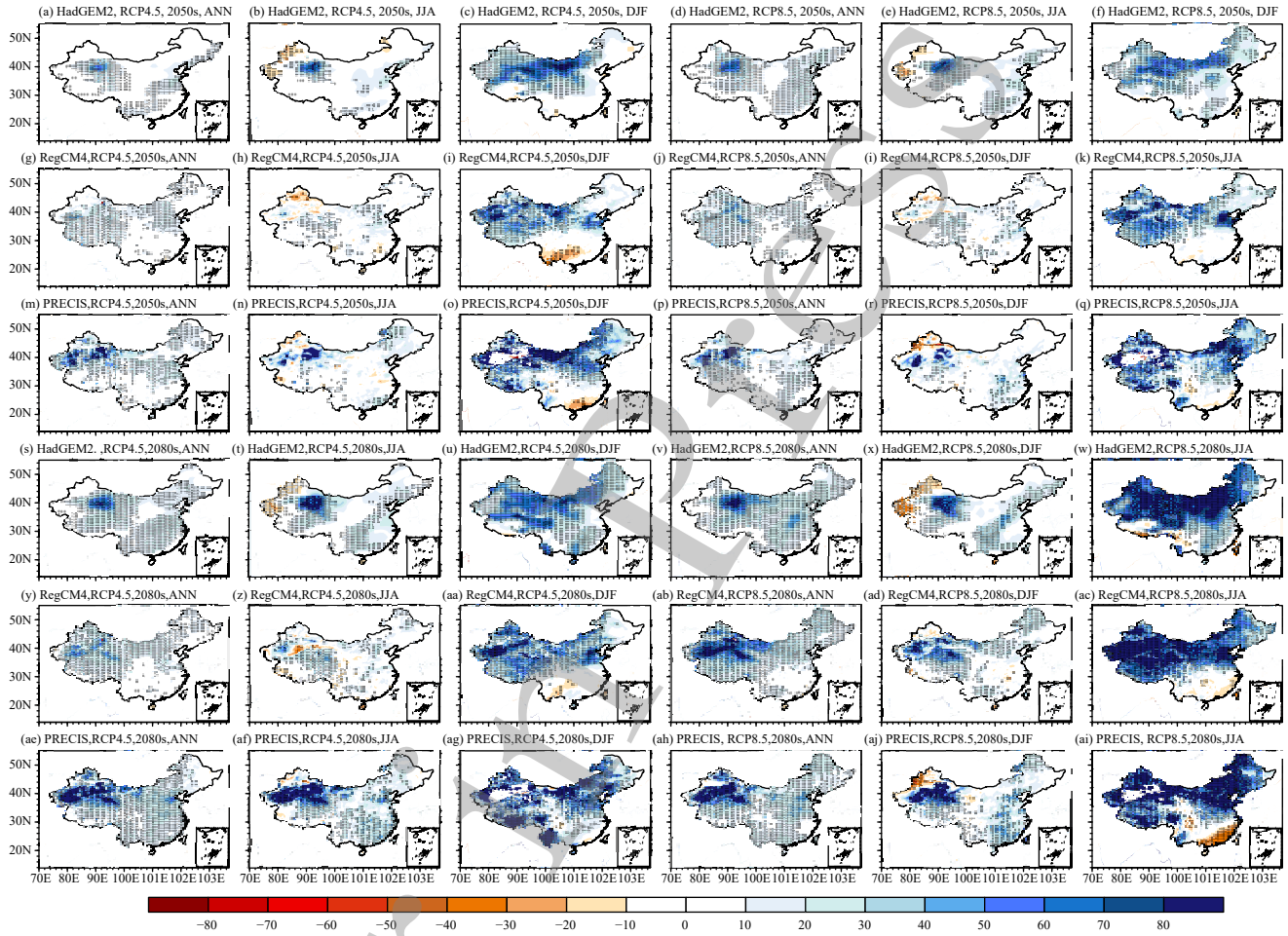


**Fig. 8.** The 30-yr (2031–2060, 2061-2090) averaged PRCPTOT compared with the baseline (1981-2010). The first column is the annual variation; the second is for June, July and August (JJA); and the third is for December, January and February (DJF). Unit: %. The areas with significant changes at the 0.95 confidence level are indicated with dots.

increase in Northwest China. The variation in summer precipitation is similar to that of the whole year, but the precipitation in some parts of NE and NW may decrease, by no more than 20%. The 2050s climate will be much wetter in the northern sub-regions like ENW and N in winter, with precipitation increasing by more than 30%. Precipitation in S and SE will decrease noticeably, especially in the RCMs projections under the RCP4.5 scenario. The increase of winter precipitation in northern parts is larger than that in the summer. By the 2080s, the spatial pattern of change is similar with that by the 2050s, while the margin of change enlarged. The annual and summer precipitation increase in NW is much more significant than that between the 2050s and baseline, and the spatial scale is wider. In winter, precipitation will increase at least by 60% in most parts above 30N under the RCP8.5 scenario. RCMs project a drier winter in the south coastal region, which is not clear present in the GCM. Under the RCP4.5 scenario, the number of wet days in the future is quite different between HadGEM2-ES and the regional models for the 2050s. HadGEM2-ES estimates fewer number of wet days in NE, little change in the central region, and more rainy days in NW. In line with the precipitation, the number of wet days in winter in N will increase in the future, while it will decrease in some parts of NE and NW. Both RegCM4 and PRECIS show a reduction in the number of wet days in S and SW (Figs. 9d-f). The three models all predict more frequent precipitation in TP. Under the RCP8.5 scenario, the Projections by the three models are consistent with those under the RCP4.5 scenario, with reduced number of wet days in S and increased number of wet days in N. The variation in precipitation intensity is mainly in the range of 0~20%. The precipitation intensity in some areas shows a slight reduction by less than 10%, such as in S under the RCP4.5 scenario, because of the precipitation decrease in S.

3.2.2 *Annual cycle*

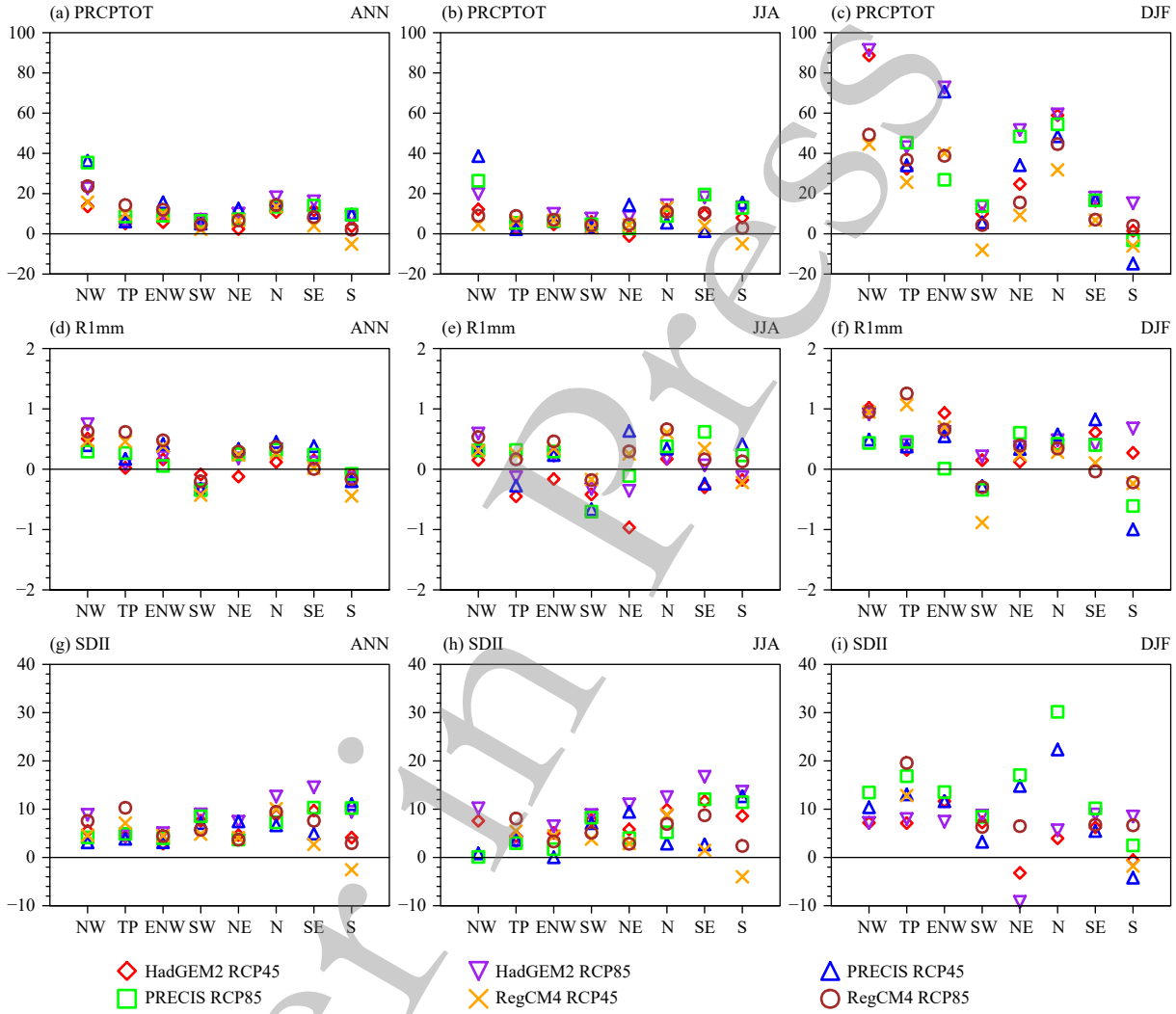


**Fig. 9.** Future variations of precipitation indexes during 2031-2060 in different sub-regions: the first column is the annual variation; the second is for JJA; and the third for is DJF. The first line is for PRCPTOT (%); the second line is for monthly average number of wet days (day); and the third line is for SDII (%). Outliers are not shown.

The climate changes in different areas exhibit different features, and the latitude-month cross-sections of climate changes averaged over the western (80°–100°E) and eastern (100°–130°E) parts of China between the baseline and the 2050s and 2080s are given in Figs. 10, 11. It can be found from Fig. 10 that precipitation will increase in more areas and last longer in the north of 37°N in the future. During March, November and December, there is a significant increase of precipitation in most areas, while the variation in S is less obvious. There is strong consistency between the results of GCMs and RCMs, and the future variations in water vapor and precipitation may be dominated by large-scale circulations and water vapor transports (Hui et al., 2018b). Under the RCP4.5 scenario, PRECIS shows the largest precipitation growth in N and a significantly more wetting tendency in winter. In the north of 32°N, the precipitation increases all the year around except for August and September, while in the south of 32°N, it is drier in January and slightly wetter in other months. The estimations by HadGEM2-ES and RegCM4 during April–September are similar to that in the historical benchmark period, basically within a margin of increase by less than 30%. It is estimated to be relatively drier in January, especially by RegCM4, and the probability reaches 30%, moreover the situation is estimated to continue until February. In addition, RegCM4 predicts that the precipitation will decrease in S during November. Under the RCP8.5 scenario, it is estimated by HadGEM2-ES that N will become wetter, while S will become drier in January. Dryness in the fall near 22–27°N simulated by RegCM4 occurs earlier and lasts longer. The estimation of PRECIS shows that precipitation near 35°N will be less than that under the RCP4.5 scenario, and precipitation increases in

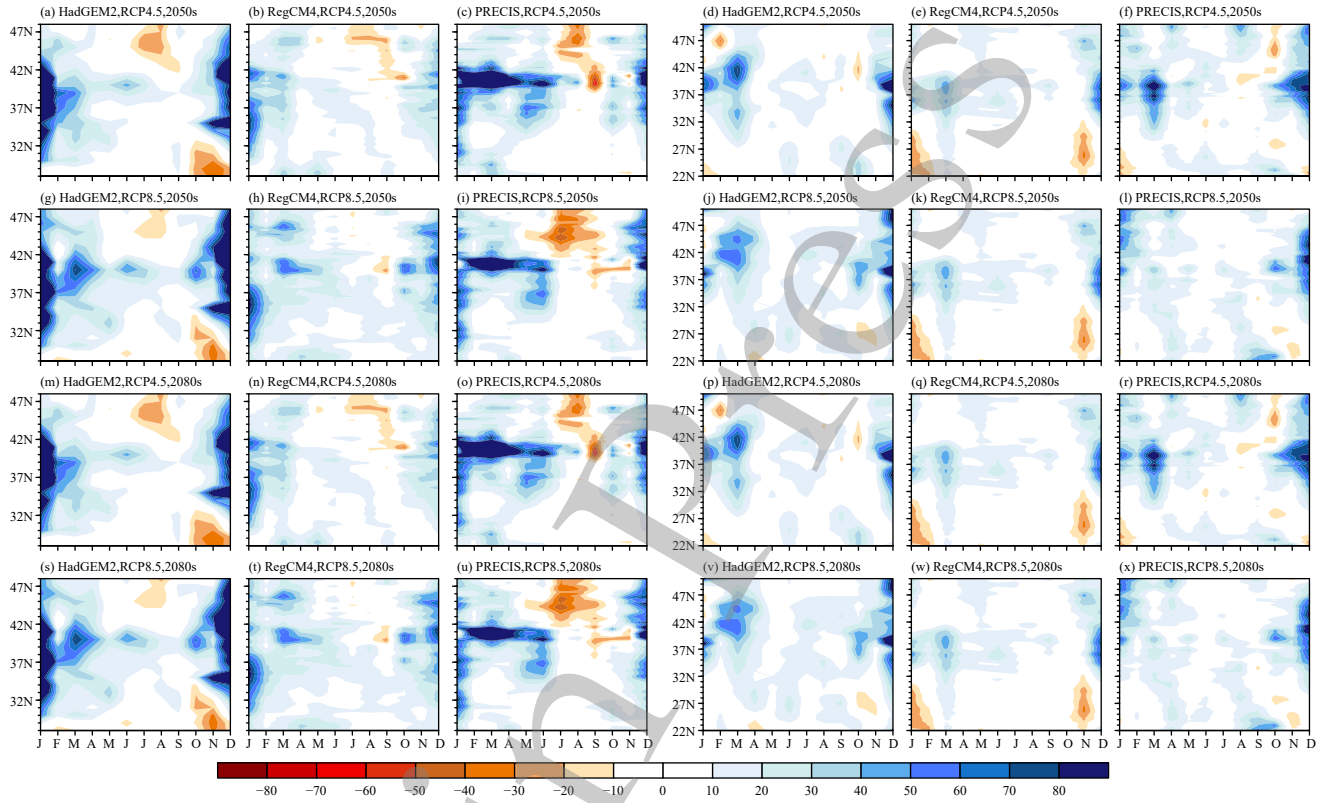


**Fig. 10.** The 30-yr (2031–2060) averaged latitude-month cross-sections of the precipitation compared with the baseline (1981–2010). The domain of left three columns are (22°–50°N, 100°–130°E), and the domain of the right three columns are (28°–48°N, 80°–100°E). Unit: %.

northern part of China. The dryness in S during January will almost disappear. For areas west of 100°E, precipitation will increase more than that east of 100°E, and the precipitation also will increase more during the winter. Chen et al. (2018) predicted that under the RCP4.5 scenario, the precipitation in N during spring and autumn will increase the most, while the precipitation in S during summer and winter will decrease.

While the precipitation increases, the number of wet days probably decreases in the future. Under both RCP4.5 and RCP8.5 scenarios, HadGEM2-ES shows a significant decrease in the number of wet days during March–September (Figs. 11a, d). However, the two RCMs still show a possible increase in the north of 37°N during May–July. The increase in the simulation by PRECIS under the RCP4.5 scenario is the largest (more than 1 day). For the area west of 100°E, the rainfall center appears northward from February to June, but this feature is not obvious in RegCM4. Overall, the changes in the number of wet days in the west part are less in the RCMs than that in the GCM, mostly within 2 days.

3.2.3 *Frequency of precipitation intensity*

The changes in the frequency of precipitation intensity under the RCP4.5 and RCP8.5 scenarios between the baseline and the 2050s are shown in Fig. 12. The results show that the light rain frequency in most sub-regions decreases, especially in NW, TP and SW. The largest decrease (by more than 3%) appears in N under the RCP4.5 scenario, as presented by PRECIS simulation. By the 2050s, rain intensity at 5–10 mm day$^{-1}$ is expected to occur more frequently in the north, with the largest increase reaching more than 1.4% in NW. While in the south, it is estimated to decrease. The growth rate of the frequency of moderate to heavy rain (10–50 mm day$^{-1}$) varies within 0–1%. And the frequency may decrease in SE and S. The frequency of heavy rain over 30 mm day$^{-1}$ is going to undergo a significant increase in S, SW and SE. By the 2050s, SE will suffer more frequent occurrences of severe storms. The decreasing frequency of light rain and the increasing frequency of heavy rain are also pointed out by Hui et al. (2018b) and Bao et al. (2015).

3.2.4 *Extreme indexes*

The changes in extreme precipitation indexes between the baseline and the 2050s and 2080s under the RCP8.5 scenarios are presented in Figs. 13, 14. The extreme wet indexes Rx5day and R95t increase in most sub-regions (Figs. 14c, d), ranging from 0 to 60% and 0 to 12%, respectively. The extreme precipitation increases as a result of the increase in occurrence frequency and intensity

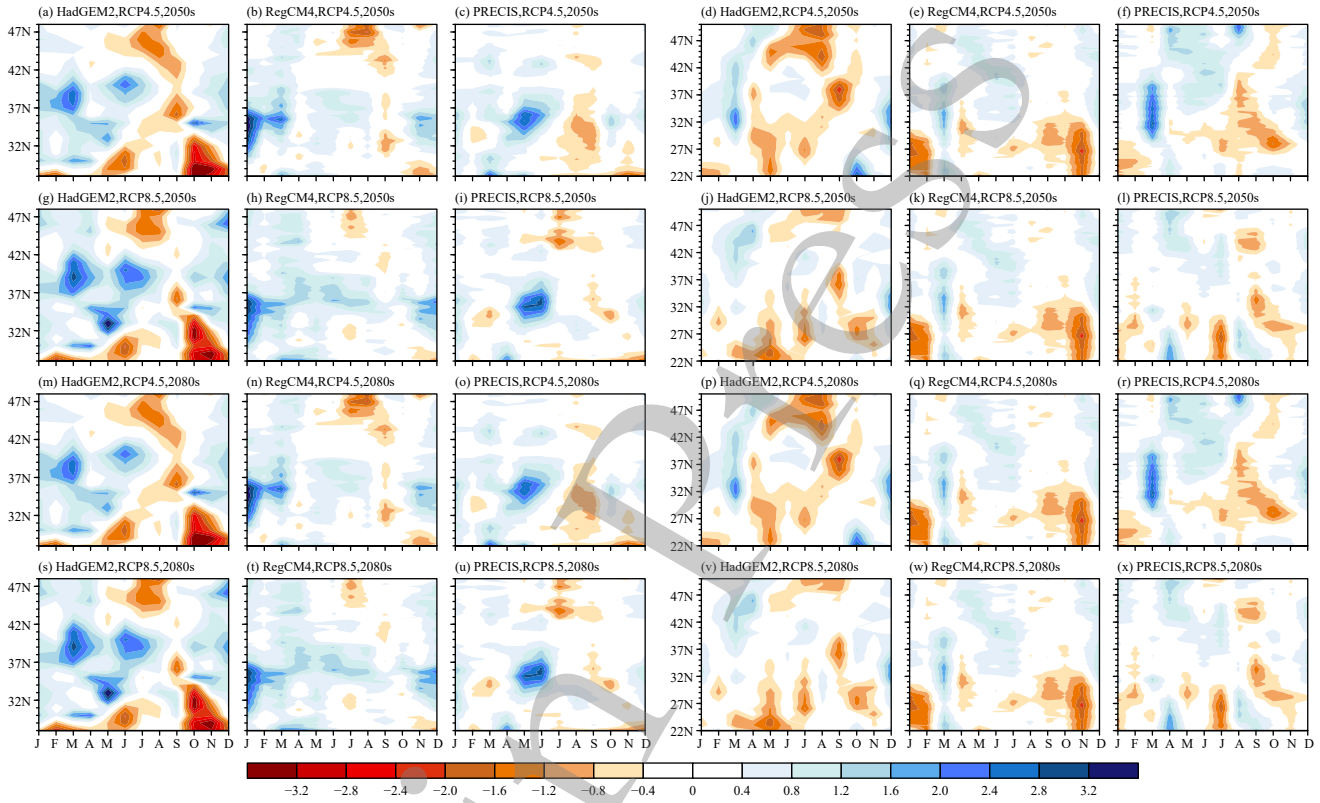


**Fig. 11.** As in Fig. 10, but for R1mm (day)$^{-1}$.

of extreme precipitation in most areas of China (Xu et al., 2019). Rx5day may increase by about 10% by the 2050s, and the return period of 50 years will be reduced to less than 10 years (Li et al., 2018本条文献指代信息不明确; Xu et al., 2018). The increase will go a step further by the 2080s, but spatial patterns are quite different across models, with HadGEM2-ES increasing most in NW and SE, RegCM4 most in west regions and PRECIS most in east regions. There are also spatial differences in other extreme indexes, indicating that result variation across different models should be considered in the projection.

The future dry season may be shortened in the arid regions. In HadGEM2-ES simulation, the dry season in NW, TP and parts of NE is shortened by 3–18 days by the 2050s and even more further shortened by the 2080s. RegCM4 estimates that the national dry season does not change much. Except for some areas, the extent of change is less than 12 days, and there is a relatively significant decrease in NW. In the simulation by PRECIS, the dry season in NW is shortened most, by more than 20 days. PRECIS' estimation in other regions is similar to RegCM4's, and the dry season in S and SE may be prolonged. CDD is expected to decrease in N (such as continental basins) but increase in the southern China (such as SE, Pearl River and Yangtze river basins) and NW (Fig. 14a), which is consistent with the existing research (Li et al., 2018本条文献指代信息不明确; Xu et al., 2019). In the future, according to HadGEM2-ES and PRECIS, there may be shorter CWDs in the southern TP and SW. RegCM4 shows that CDD may extend in some areas of the southern China except the SW.

The possible factors that control the change of mean precipitation are firstly investigated by analyzing the changes of total water vapor flux and divergence at 850 hPa (Fig. 15). The precipitation is supposed to increase in most areas of China by the 2050s, while decrease in the south part in winter (Fig. 8). In a warmer future, there will be a higher water content in the atmosphere, making more water vapor flux over almost whole China. The increases of water vapor flux are much greater in the East China, resulting in larger increases of precipitation. In the south of China, the increase of water vapor flux is relatively small. RegCM4 produces relatively larger increases of water vapor flux than PRECIS along the east coast of China, which can explain the precipitation increases in Fig. 8.

Figure 16 shows the scatter diagrams of extreme precipitation indexes against various climate variables. All the four extreme precipitation indexes are sensitive to PRCPTOT. There is a negative correlation between the dry index CDD and PRCPTOT, and positive correlations

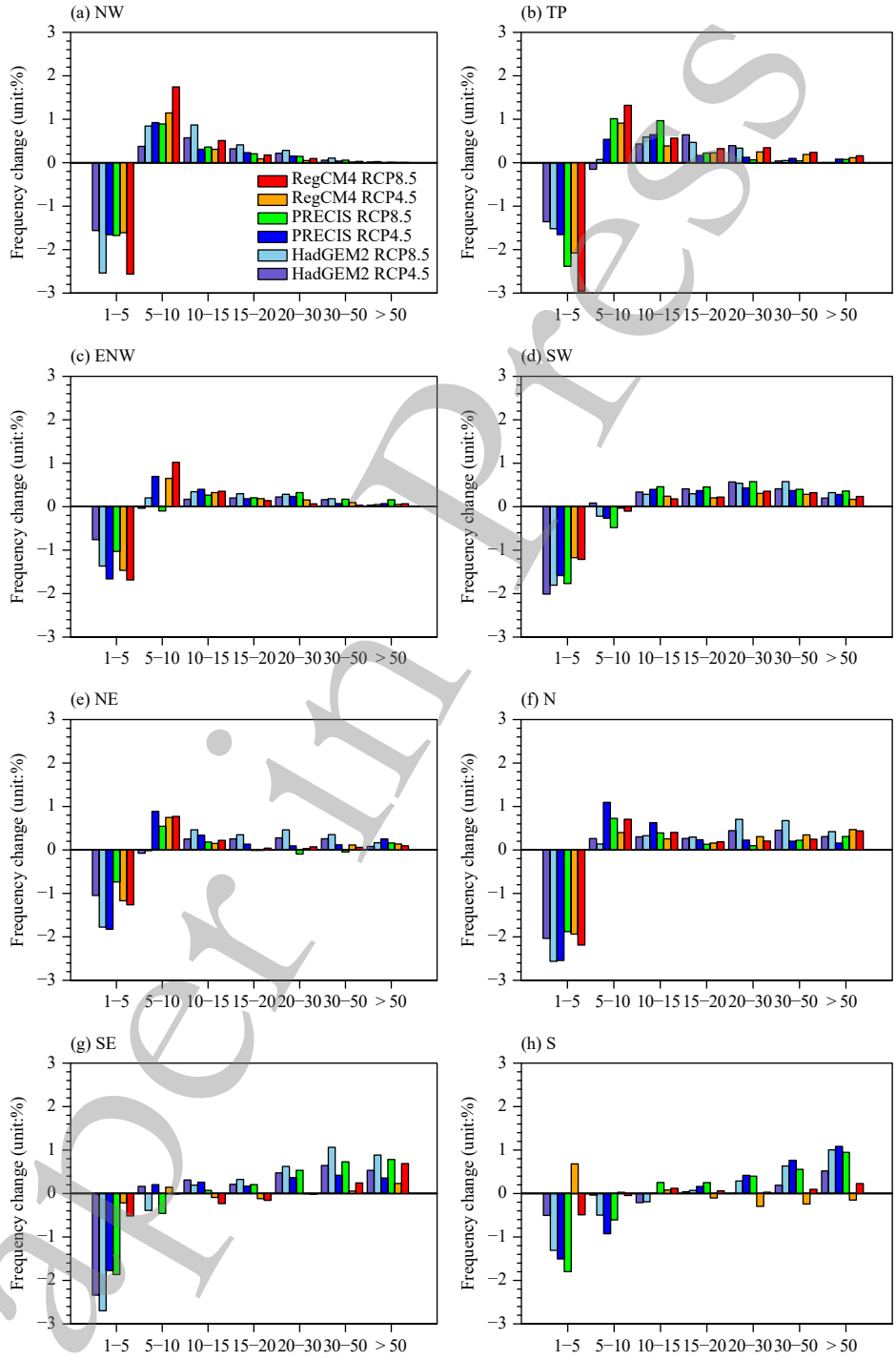


**Fig. 12.** Changes in the frequency of daily precipitation intensity in different sub-regions over China.

between the wet indexes and PRCPTOT. Because of the close relationship between precipitation and moisture, the extreme indexes have high correlations with water vapor flux except CWD for which the correlation is relatively weaker. Wind at 850 hPa does not show noticeable impact on extreme indexes, except meridional wind in RegCM4. The wet indexes of Rx5day and R95t have positive correlations with meridional wind. To conclude, stronger summer monsoons (positive v-wind increases) transport more moisture to China, leading to more precipitation and resulting in an increase in extreme precipitation indexes.

## 4. Conclusions and discussion

As the temperature may rise in the future, the poten-

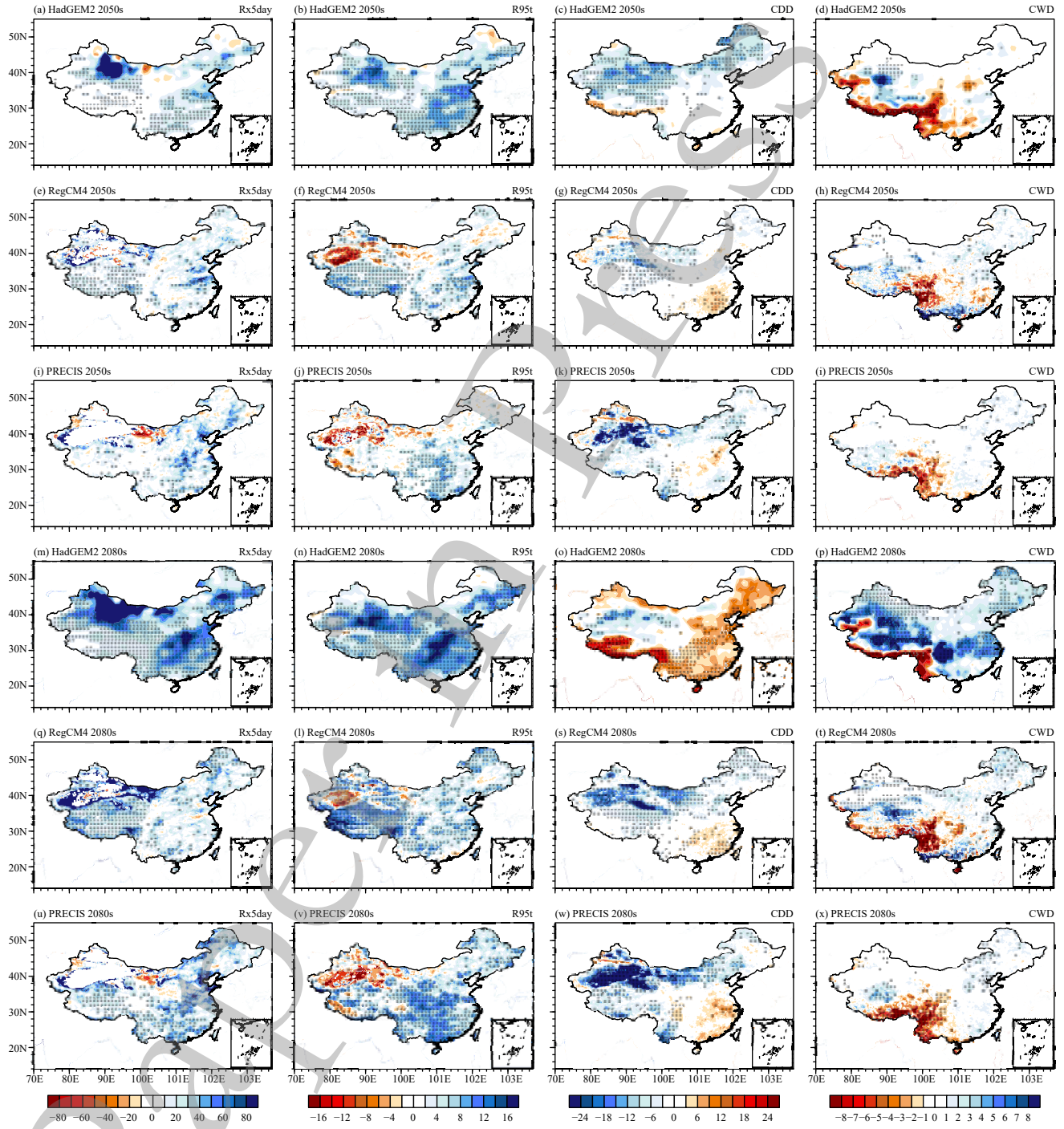


**Fig. 13.** The 30-yr (2031–2060 and 2061–2090) averaged annual extreme indexes compared with the baseline (1981–2010). The first column is for Rx5day (%); the second column is for R95t (%); the third column is for CDD (day); and the fourth column is for CWD (day). The areas with significant changes at the 0.95 confidence level are indicated with black dots.

tial risk for floods and droughts in China is also increasing. The existing literature has shown that future flood disasters would exhibit different degrees of aggravation under different scenarios, with the highest increase trend under highest level of $CO_2$ concentrations (Liang et al., 2019). Previous studies have also highlighted that there is still a lot of uncertainty in predicting the climate change in a region with a complex terrain, unique climate and climate systems like China (Gu et al., 2018; Chen and Gao, 2019). This background underscores the importance of in-depth analyses of high-resolution and multiple RCM simulations to build more robust and reliable climate change scenarios for a large country as China.

In this paper, we employ two RCMs, i.e. RegCM4 and

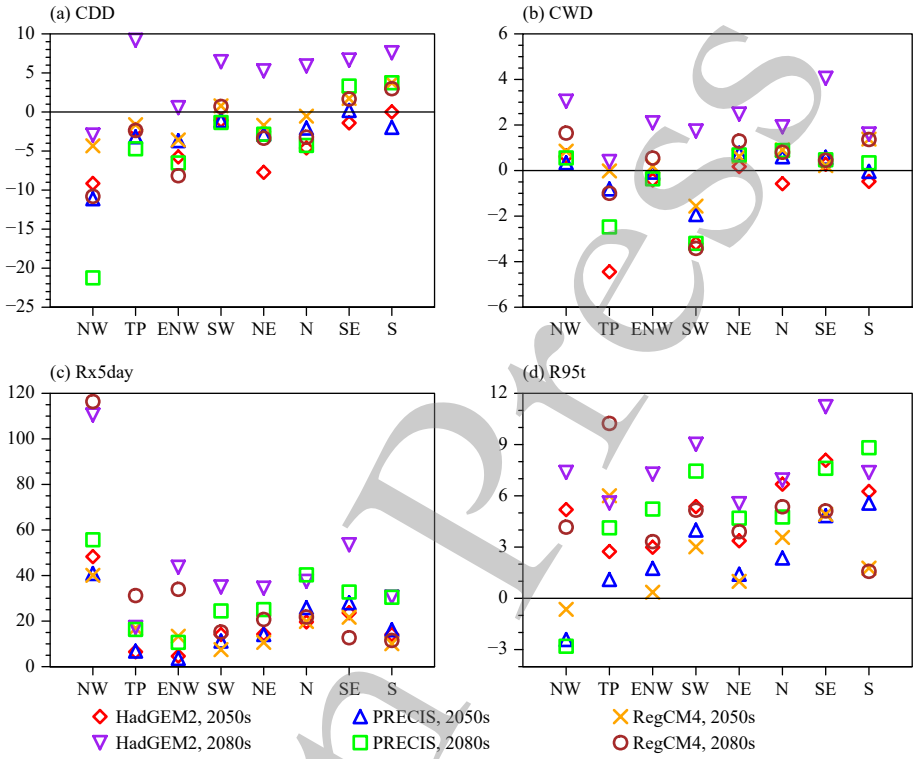


**Fig. 14.** Future changes of extreme indexes in different sub-regions under RCP8.5 for (a) CDD, (b) CWD (day), (c) Rx5day (%) and (d) R95t (%). Outliers are not shown.

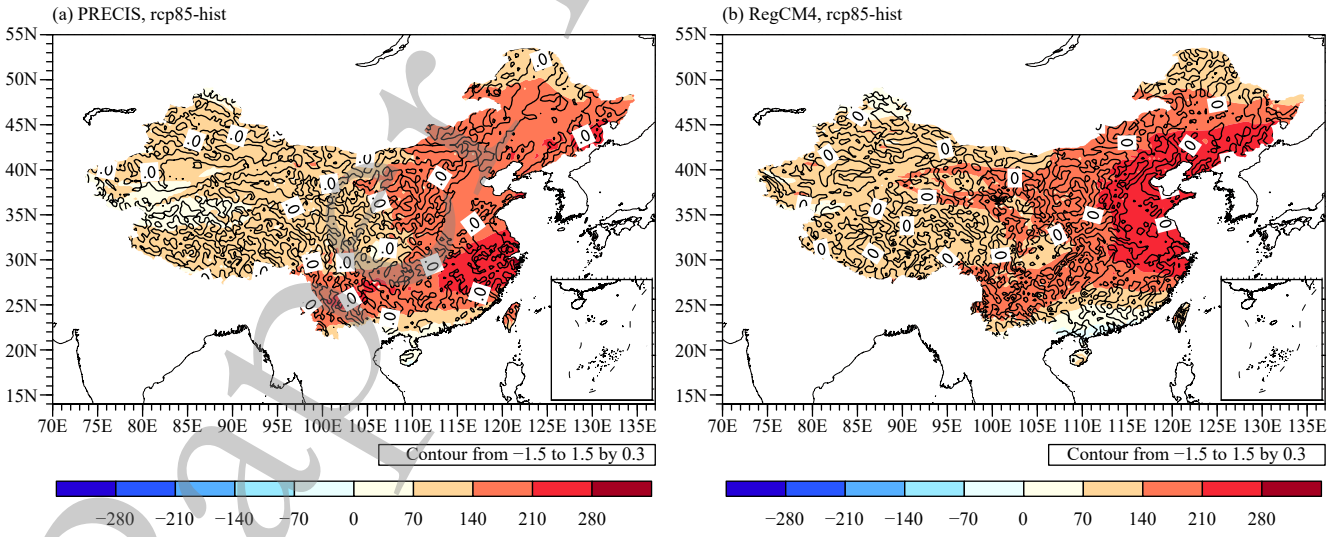


**Fig. 15.** Changes of the total water vapor flux integrated from 1000 to 200 hPa (shading; g·s kg$^{-1}$) and the divergence at 850 hPa (contour; 10–6 s$^{-1}$) over the period of 2031–2060 under the RCP8.5 scenario.

PRECIS, being driven by the GCM (HadGEM2-ES), to detect changes in mean and extreme precipitation in China between the baseline climatology of 1981–2010 and the future climatology of 2031–2060 and 2061–2090, respectively. Firstly, the simulation abilities of the three models are evaluated by comparing with the observation data of 1986–2005. Then the climate change Projections by different models for 2031–2060 and 2061–2090 under the RCP4.5 and RCP8.5 scenarios are analyzed and compared with the reanalysis data of the baseline 1981-2010 climatology. The results provide an improved reference for future climate response and disaster prevention.

The performance evaluation of PRECIS and RegCM4 based on observation data shows that both models can simulate precipitation and related extreme indexes, and

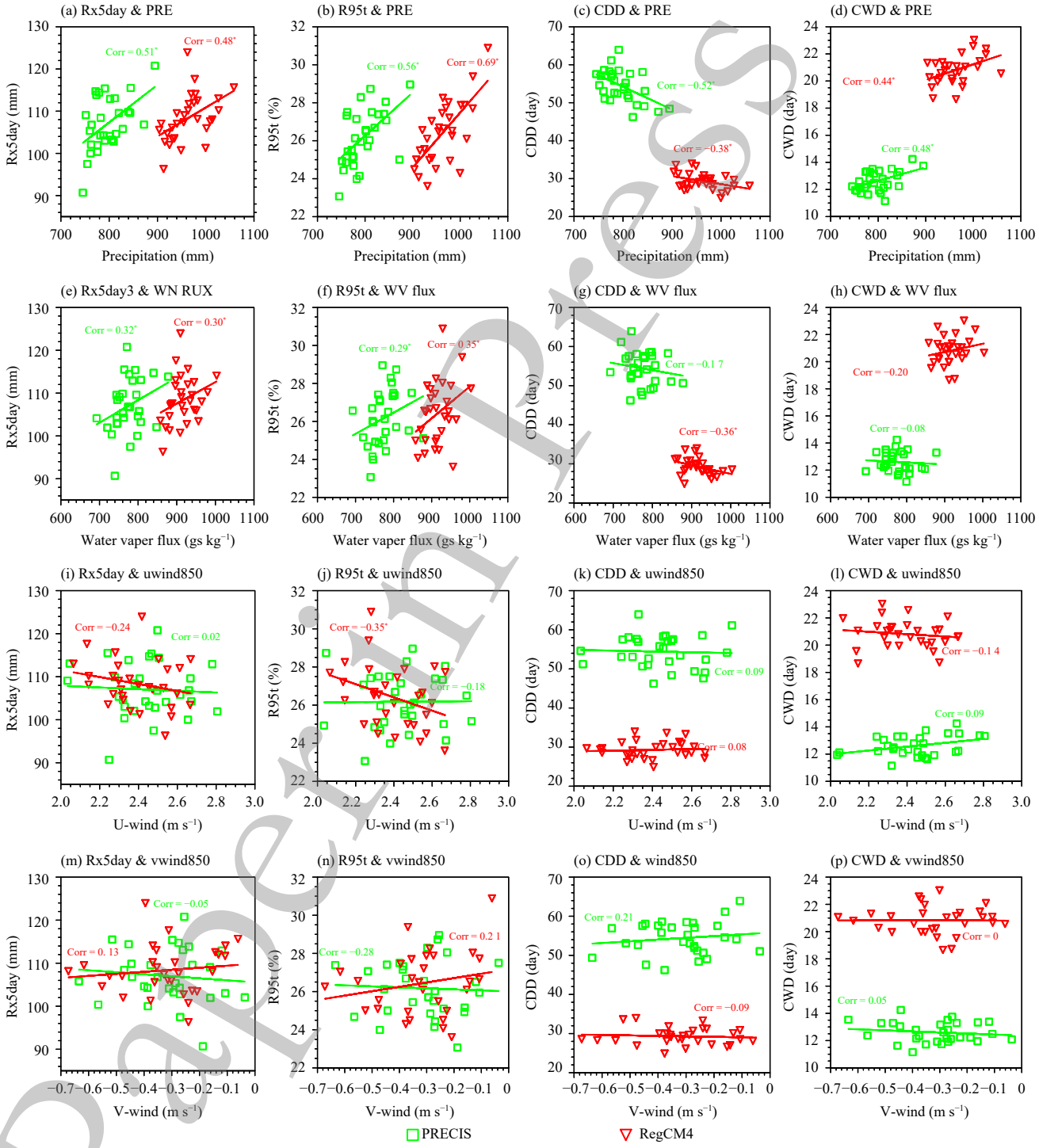


**Fig. 16.** Scatter diagrams of the extreme precipitation indexes Rx5day (a–d), R95t (e–h), CDD (i–l) and CWD (m–p) against the annual mean precipitation, total water vapor flux integrated between 1000–200 hPa, zonal and meridional winds as well as the linear regressions under the RCP8.5 scenario. The variables cover the period of 2031–2060 and are averaged over China. Corr means correlation coefficient, * means passing the 0.1 significance test.

reproduce their spatial distribution. Compared with HadGEM2-ES, the two regional models can better represent the fine physical process by improving the resolution. They can also provide reliable spatial patterns of extreme precipitation, and their simulations have a high spatial correlation with the observations (Gu et al., 2018). In most parts of China, the three models overestimate the annual total precipitation, especially in NW and TP, which are areas with less precipitation (Yu et al., 2020). In humid areas such as SE and S, the simulation is good,

and the bias is mainly below 20%. In most regions, RCMs can outperform HadGEM2-ES by increasing the correlations with observations and reducing RMSE. However, the RCMs perform poorly in N. For other indicators, the performances of RCMs are comparable, with the smallest bias in SE, and large biases in NW and inland areas. Except for PRECIS which underestimates multiple indicators in NW, the negative bias mainly occurs in the wet zone. It is worth noting that for most indicators at least one of the two RCMs usually outperforms HadGEM2-ES. The AV of RCMs is more obvious in the western China, lithely attributable to the improved depiction of complex terrain herein.

Of course, the performances of two RCMs are not perfect, and there are still some biases in comparison with the observations. Part of the bias comes from the GCM, and part comes from the RCM itself. For example, the GCM overestimates the annual precipitation on the eastern edge of the Qinghai-Tibet Plateau and the southwest border of China, and brings the biases into the RCM. Similar conclusions are found in many studies on GCM and RCM assessments (Flato et al., 2013; Bao et al., 2015). The GCM is more likely to overestimate the precipitation in Northeast China, and the two RCMs further aggravate the bias of annual precipitation in Northeast China, especially the RegCM4 model. Some studies (Gao et al., 2016; Yu et al., 2020) also found that even when the so called "perfect boundary condition", i.e. reanalysis dataset, is used to drive RegCM4, the annual precipitation simulated by RegCM4 in Northeast China still shows a positive bias. It may be due to the positive vorticity deviation in the lower levels of Northeast China (Hui et al., 2018b), or may be related to the deficiency of parameterization scheme of physical processes.

Projections of climate change between the baseline and the future climate of the 2050s and 2080s are made under the RCP4.5 and RCP8.5 scenarios. The results show a trend of increase in the climatology-averaged annual precipitation in NW, NE, SE and other regions of China, most significantly in the Turpan Basin. The increase in the annual precipitation is mainly due to the precipitation increase in winter and summer. Regardless of absolute precipitation, the growth rate in DJF is higher than in JJA in most regions. In the future, the increase of water vapor fluxes in S will lead to the enhancement of extreme precipitation in the monsoon sub-region (Park and Min, 2018). To a large extent, the average change of climate depends on the driving GCMs. And according to HadGEM2-ES, it is expected to be wetter in the future, and RCMs produce more regional details. Compared with RegCM4, PRECIS predicts heavier precipitation in TP and NW during summer. The variation range of precipitation in the northern China is larger than that in the south, consistent with previous studies (Gu et al., 2018; Sun et al., 2018). The number of wet days also increases in NW, but it shows a decreasing trend in S. Moreover, its future increasement shows a reduction trace from north to south. It suggests that areas with insufficient rainfall in the baseline climate are likely to become wetter in the future, but the precipitation intensity will not change much. Light precipitation (1-5 mm day$^{-1}$) will decrease in almost all simulations. In NW and TP, moderate precipitation (5-10 mm day$^{-1}$) will increase most, while in SE and S, heavy precipitation (> 30 mm day$^{-1}$) will do so. In areas with abundant precipitation, the extreme precipitation events will become more frequent, thus raising the risk of floods (Li et al., 2018本条文献指代信息不明确). The Projection results are consistent with previous studies to some extent (Bao et al., 2015; Niu et al., 2017; Chen and Gao, 2019).

The impact that changes in climate extremes exert on agriculture, hydrology and human health is closely related to the mitigation ability of the society, which is, by a large extent, determined by the level of social development. The warming trend and precipitation variability may lead to increasing disparity in water availability across China. If other variables, such as land use and land cover change (Avila et al., 2012) and aerosol emissions (Wang et al., 2016), are taken into account, it will be predicted that climate extremes will become more variable across different locations. The potential impact of such dynamics on water resources and water uses should be considered when China is taking measures to mitigate and adapt to climate change, including institutional, political structural and legal framework measures (Yang et al., 2018). The more accurate Projection of climate extremes requires considering the integrated climate impacts (Niu et al., 2017). There are great uncertainties in the simulation and Projection of future climate change, especially at the regional and local scales, and multi-model integrated climate Projection is an important and effective method to reduce these uncertainties (Giorgi et al., 2009).

The climate projections provided in this study can facilitate the efforts of climate service institutions in providing innovative long-term advisory services and can help local governments to design climate-smart decisions. In addition, these high-resolution long-term regional climate Projection data can be directly incorporated into the existing climate service tools to improve simulation accuracies and thus better informing local governments, businesses, and other stakeholders with re-

gard to climate risk assessment and management.

***Acknowledgments.*** We thank Dr. Ying Xu from National Climate Centre (NCC) of China Meteorological Administration (CMA) for providing RegCM4 datasets. We also thank Dr. Jia Wu from NCC of CMA and Dr. Xuejie Gao from Institute of Atmospheric Physics of Chinese Academy of Sciences for providing the CN05.1 gridded dataset. We also thank Nanjing Hurricane Translation for reviewing the English language quality of this paper.

## REFERENCES

Avila, F. B., A. J. Pitman, M. G. Donat, et al., 2012: Climate model simulated changes in temperature extremes due to land cover change. *J. Geophys. Res. Atmos.*, **117**, D04108, doi: 10.1029/2011JD016382.

Bao, J. W., J. M. Feng, and Y. L. Wang, 2015: Dynamical downscaling simulation and future projection of precipitation over China. *J. Geophys. Res. Asmos.*, **120**, 8227–8243, doi: 10.1002/2015JD023275.

Chen, H. P., 2013: Projected change in extreme rainfall events in China by the end of the 21st century using CMIP5 models. *Chinese Sci. Bull.*, **58**, 743–752, doi: 10.1007/s11434-012-5612-2. (in Chinese)

Chen, L., Z. G. Ma, Z. H. Li, et al., 2018: Dynamical downscaling of temperature and precipitation extremes in China under current and future climates. *Atmos. Ocean*, **56**, 55–70, doi: 10.1080/07055900.2017.1422691.

Chen, N., and X. J. Gao, 2019: Climate change in the twenty-first century over China: Projections by an RCM and the driving GCM. *Atmos. Oceanic Sci. Lett.*, **12**, 270–277, doi: 10.1080/16742834.2019.1612695.

Di Luca, A., R. de Elía, and R. Laprise, 2013: Potential for small scale added value of RCM's downscaled climate change signal. *Climate Dyn.*, **40**, 601–618, doi: 10.1007/s00382-012-1415-z.

Dosio, A., H.-J. Panitz, M. Schubert-Frisius, et al., 2015: Dynamical downscaling of CMIP5 global circulation models over CORDEX-Africa with COSMO-CLM: Evaluation over the present climate and analysis of the added value. *Climate Dyn.*, **44**, 2637–2661, doi: 10.1007/s00382-014-2262-x.

Duan, W. L., N. Hanasaki, H. Shiogama, et al., 2019: Evaluation and future projection of Chinese precipitation extremes using large ensemble high-resolution climate simulations. *J. Climate*, **32**, 2169–2183, doi: 10.1175/jcli-d-18-0465.1.

Feser, F., B. Rockel, H. von Storch, et al., 2011: Regional climate models add value to global model data: A review and selected examples. *Bull. Amer. Meteor. Soc.*, **92**, 1181–1192, doi: 10.1175/2011BAMS3061.1.

Flato, G., J. Marotzke, B. Abiodun, et al., 2013: Evaluation of climate models. *Climate Change 2013: The Physical Science Basis. Contribution of Working Group I to the Fifth Assessment Report of the Intergovernmental Panel on Climate Change*, T. F. Stocker, D. Qin, G.-K. Plattner, et al., Eds., Cambridge University Press, Cambridge, UK.

Gao X.-J., M.-L. Wang, and F. Giorgi, 2013: Climate change over China in the 21st century as simulated by BCC_CSM1.1-RegCM4.0. Atmos. *Oceanic Sci. Lett.*, **6**, 381–386, doi: 10.3878/j.issn.1674-2834.13.0029.

Gao, X.-J., Y. Shi, and F. Giorgi, 2016: Comparison of convective parameterizations in RegCM4 experiments over China with CLM as the land surface model. *Atmos. Oceanic Sci. Lett.*, **9**, 246–254, doi: 10.1080/16742834.2016.1172938.

Gao, X. J., Y. Shi, Z. Y. Han, et al., 2017: Performance of RegCM4 over major river basins in China. *Adv. Atmos. Sci.*, **34**, 441–455, doi: 10.1007/s00376-016-6179-7.

Gao, X.-J., J. Wu, Y. Shi, et al., 2018: Future changes in thermal comfort conditions over China based on multi-RegCM4 simulations. *Atmos. Oceanic Sci. Lett.*, **11**, 291–299, doi: 10.1080/16742834.2018.1471578.

Giorgi, F., 2019: Thirty years of regional climate modeling: Where are we and where are we going next? *J. Geophys. Res. Atmos.*, **124**, 5696–5723, doi: 10.1029/2018JD030094.

Giorgi, F., C. Jones, and G. R. Asrar, 2009: Addressing climate information needs at the regional level: The CORDEX framework. *WMO Bull.*, **58**, 175–183.

Gu, H. H., Z. B. Yu, G. L. Wang, et al., 2015: Impact of climate change on hydrological extremes in the Yangtze River Basin, China. *Stoch. Environ. Res. Risk Assess.*, **29**, 693–707, doi: 10.1007/s00477-014-0957-5.

Gu, H. H., Z. B. Yu, C. H. Yang, et al., 2018: High-resolution ensemble projections and uncertainty assessment of regional climate change over China in CORDEX East Asia. *Hydrol. Earth Syst. Sci.*, **22**, 3087–3103, doi: 10.5194/hess-22-3087-2018.

Guo, J. H., G. H. Huang, X. Q. Wang, et al., 2018: Future changes in precipitation extremes over China projected by a regional climate model ensemble. *Atmos. Environ.*, **188**, 142–156, doi: 10.1016/j.atmosenv.2018.06.026.

Han, Z. Y., X. J. Gao, Y. Shi, et al., 2015: Development of Chinese high resolution land cover data for the RegCM4/CLM and its impact on regional climate simulation. *J. Glaciol. Geocryol.*, **374**, 857–866, doi: 10.7522/j.issn.1000-0240.2015.0095. (in Chinese)

Han, Z. Y., Y. X. Wang, and Y. Nie, 2016: The radiation budget in a regional climate simulation by RegCM4 for eastern China. *Trans. Atmos. Sci.*, **39**, 683–691, doi: 10.13878/j.cnki.dqkxxb.20151104001. (in Chinese)

Han, Z. Y., B. T. Zhou, Y. Xu, et al., 2017: Projected changes in haze pollution potential in China: An ensemble of regional climate model simulations. *Atmos. Chem. Phys.*, **17**, 10109–10123, doi: 10.5194/acp-17-10109-2017.

Holtslag, A. A. M., E. I. F. De Bruijn, and H.-L. Pan, 1990: A high resolution air mass transformation model for short-range weather forecasting. *Mon. Wea. Rev.*, **118**, 1561–1575, doi: 10.1175/1520-0493(1990)118<1561:AHRAMT>2.0.CO;2.

Hui, P. H., J. P., Tang, S. Y., Wang, et al, 2018a: Climate change projections over China using regional climate models forced by two CMIP5 global models. Part I: Evaluation of historical simulations. *Int. J. Climatol.*, **38**, e57–e77, doi: 10.1002/joc.5351.

Hui, P. H., J. P., Tang, S. Y., Wang, et al, 2018b: Climate change projections over China using regional climate models forced by two CMIP5 global models. Part II: Projections of future climate. *Int. J. Climatol.*, **38**, e78–e94, doi: 10.1002/joc.5409.

Jones, C. D., J. K. Hughes, N. Bellouin, et al., 2011: The HadGEM2-ES implementation of CMIP5 centennial simulations. *Geosci. Model Dev.*, **4**, 543–570, doi: 10.5194/gmd-4-543-2011.

Kiehl, J. T., J. J. Hack, G. B. Bonan, et al., 1998: The national center for atmospheric research community climate model: CCM3. *J. Climate*, **11**, 1131–1149, doi: 10.1175/1520-0442(1998)011<1131:TNCFAR>2.0.CO;2.

Li, D. H., L. W. Zou, and T. J. Zhou, 2018: Extreme climate event changes in China in the 1.5 and 2°C Warmer Climates: Results from statistical and dynamical downscaling. *J. Geophys. Res. Atmos.*, **123**, 10215–10230, doi: 10.1029/2018jd028835.

Li, H. X., H. P. Chen, H. J. Wang, et al., 2018: Future precipitation changes over China under 1.5°C and 2.0°C global warming targets by using CORDEX regional climate models. *Sci. Total Environ.*, **640–641**, 543–554, doi: 10.1016/j.scitotenv.2018.05.324.

Li, P. X., K. Furtado, T. J. Zhou, et al., 2018: The diurnal cycle of East Asian summer monsoon precipitation simulated by the Met Office Unified Model at convection-permitting scales. *Climate Dyn.*, **11**, 7, doi: 10.1007/s00382-018-4368-z.

Li, W., Z. H. Jiang, J. J. Xu, et al., 2016: Extreme precipitation indices over China in CMIP5 models. Part II: Probabilistic projection. *J. Climate*, **29**, 8989–9004, doi: 10.1175/JCLI-D-16-0377.1.

Liang, Y. L., Y. L. Wang, Y. J. Zhao, et al., 2019: Analysis and projection of flood hazards over China. *Water*, **11**, 1022, doi: 10.3390/w11051022.

Lu, C., G. H. Huang, and X. Q. Wang, 2019: Projected changes in temperature, precipitation, and their extremes over China through the RegCM. *Climate Dyn.*, **53**, 5859–5880, doi: 10.1007/s00382-019-04899-7.

Niu, X. R., S. Y. Wang, J. P. Tang, et al., 2017: Ensemble evaluation and projection of climate extremes in China using RMIP models. *Int. J. Climatol.*, **38**, 2039–2055, doi: 10.1002/joc.5315.

Pal, J. S., F. Giorgi, X. Q. Bi, et al., 2007: Regional climate modeling for the developing world: The ICTP RegCM3 and RegCNET. *Bull. Amer. Meteor. Soc.*, **88**, 1395–1410, doi: 10.1175/BAMS-88-9-1395.

Park, C., and S.-K. Min, 2018: Multi-RCM near-term projections of summer climate extremes over East Asia. *Climate Dyn.*, **52**, 4937–4952, doi: 10.1007/s00382-018-4425-7.

Shi, Y., G. L. Wang, and X. J. Gao, 2018: Role of resolution in regional climate change projections over China. *Climate Dyn.*, **51**, 2375–2396, doi: 10.1007/s00382-017-4018-x.

Sun, H. M., A. Q. Wang, J. Q. Zhai, et al., 2018: Impacts of global warming of 1.5°C and 2.0°C on precipitation patterns in China by regional climate model (COSMO-CLM). *Atmos. Res.*, **203**, 83–94, doi: 10.1016/j.atmosres.2017.10.024.

Sun, Q. H., C. Y. Miao, and Q. Y. Duan, 2016: Extreme climate events and agricultural climate indices in China: CMIP5 model evaluation and projections. *Int. J. Climatol.*, **36**, 43–61, doi: 10.1002/joc.4328.

Taylor, K. E., 2001: Summarizing multiple aspects of model performance in a single diagram. *J. Geophys. Res. Atmos.*, **106**, 7183–7192, doi: 10.1029/2000JD900719.

Wang, L., and W. Chen, 2014: A CMIP5 multimodel projection of future temperature, precipitation, and climatological drought in China. *Int. J. Climatol.*, **34**, 2059–2078, doi: 10.1002/joc.3822.

Wang, Z. L., L. Lin, M. L. Yang, et al., 2016: The effect of future reduction in aerosol emissions on climate extremes in China. *Climate Dyn.*, **47**, 2885–2899, doi: 10.1007/s00382-016-3003-0.

Webster, P. J., V. O. Magaña, T. N. Palmer, et al., 1998: Monsoons: Processes, predictability, and the prospects for prediction. *J. Geophys. Res. Oceans*, **103**, 14451–14510, doi: 10.1029/97JC02719.

Wei P. P., G. T. Dong, J. Shi, et al., 2019: Dynamical downscaling simulation and projection of extreme precipitation over East China. *Climatic Environ. Res.*, **24**, 86–104, doi: 10.3878/j.issn.1006-9585.2018.17169. (in Chinese)

Wilson, S., D. Hassell, D. Hein, et al., 2015: Technical Manual for PRECIS: The Met Office Hadley Centre Regional Climate Modelling System Version 2.0.0. Met Office Hadley Centre. (查阅所有网上资料，未找到报告编号及出版地信息，请联系作者补充)

Wu, J., and X.-J. Gao, 2013: A gridded daily observation dataset over China region and comparison with the other datasets. *Chinese J. Geophys.*, **56**, 1102–1111, doi: 10.6038/cjg20130406. (in Chinese)

Xu, K., B. B. Xu, J. L. Ju, et al., 2019: Projection and uncertainty of precipitation extremes in the CMIP5 multimodel ensembles over nine major basins in China. *Atmos. Res.*, **226**, 122–137, doi: 10.1016/j.atmosres.2019.04.018.

Xu, Y., X. J. Gao, Y. Shen, et al., 2009: A daily temperature dataset over China and its application in validating a RCM simulation. *Adv. Atmos. Sci.*, **26**, 763–772, doi: 10.1007/s00376-009-9029-z.

Xu, Y., X. J. Gao, F. Giorgi, et al., 2018: Projected changes in temperature and precipitation extremes over China as measured by 50-yr return values and periods based on a CMIP5 ensemble. *Adv. Atmos. Sci.*, **35**, 376–388, doi: 10.1007/s00376-017-6269-1.

Yang, H., Z. H. Jiang, and L. Li, 2016: Biases and improvements in three dynamical downscaling climate simulations over China. *Climate Dyn.*, **47**, 3235–3251, doi: 10.1007/s00382-016-3023-9.

Yang, X., E. F. Wood, J. Sheffield, et al., 2018: Bias correction of historical and future simulations of precipitation and temperature for China from CMIP5 models. *J. Hydrometeor.*, **19**, 609–623, doi: 10.1175/jhm-d-17-0180.1.

Yu, K., P. H. Hui, W. D. Zhou, et al., 2020: Evaluation of multi‐RCM high‐resolution hindcast over the CORDEX East Asia Phase II region: Mean, annual cycle and interannual variations. *Int. J. Climatol.*, **40**, 2134–2152, doi: 10.1002/joc.6323.

Yu, Z. B., H. H. Gu, J. G. Wang, et al., 2018: Effect of projected climate change on the hydrological regime of the Yangtze River Basin, China. *Stoch. Environ. Res. Risk Assess.*, **32**, 1–16, doi: 10.1007/s00477-017-1391-2.

Yun, Y. X., C. H. Liu, Y. L. Luo, et al., 2020: Convection-permitting regional climate simulation of warm-season precipitation over Eastern China. *Climate Dyn.*, **54**, 1469–1489, doi: 10.1007/s00382-019-05070-y.

Zhang, D. F., Z. Y. Han, and Y. Shi, 2017: Comparison of climate projection between the driving CSIRO-Mk3.6.0 and the

downscaling simulation of RegCM4.4 over China. *Climate Change Res.*, **13**, 557–568, doi: 10.12006/j.issn.1673-1719.2017.101. (in Chinese)

Zhang, L. X., P. L. Wu, T. J. Zhou, et al., 2016: Added value of high resolution models in simulating global precipitation characteristics. *Atmos. Sci. Lett.*, **17**, 646–657, doi: 10.1002/asl.715.

Zhou, B. T., Q. Z. Wen, Y. Xu, et al., 2014: Projected changes in temperature and precipitation extremes in china by the CMIP5 multimodel ensembles. *J. Climate*, **27**, 6591–6611, doi: 10.1175/JCLI-D-13-00761.1.

Zhou, B. T., Z. Y. Wang, Y. Shi, et al., 2018: Historical and future changes of snowfall events in China under a warming background. *J. Climate*, **31**, 5873–5889, doi: 10.1175/JCLI-D-17-0428.1.

Zhou, P., and Z. Y. Liu, 2018: Likelihood of concurrent climate extremes and variations over China. *Environ. Res. Lett.*, **13**, 094023, doi: 10.1088/1748-9326/aade9e.本条文献在正文中未被引用

Zhu, J. X., G. Huang, X. Q. Wang, et al., 2017: High-resolution projections of mean and extreme precipitations over China through PRECIS under RCPs. *Climate Dyn.*, **50**, 4037–4060, doi: 10.1007/s00382-017-3860-1.